

Enhanced canonical Wnt signaling during early zebrafish development perturbs the interaction of cardiac mesoderm and pharyngeal endoderm and causes thyroid specification defects

Isabelle Vandernoot^{1,*}, Benoît Haerlingen^{1,*}, Achim Trubiroha^{1,2}, Pierre Gillotay¹, Véronique Janssens¹, Robert Opitz^{1,3,#} and Sabine Costagliola^{1,#}

¹ Institute of Interdisciplinary Research in Molecular Human Biology (IRIBHM), Université Libre de Bruxelles, Route de Lennik 808, 1070 Brussels, Belgium.

² German Federal Institute for Risk Assessment (BfR), Department Chemicals and Product Safety, Max-Dohrn-Strasse 8-10, 10589, Berlin, Germany.

³ Institute of Experimental Pediatric Endocrinology, Charité Universitätsmedizin Berlin, Augustenburger Platz 1, 13353, Berlin, Germany.

* These authors contributed equally to this work.

These authors contributed equally to this work.

Author Contact Details:

Isabelle Vandernoot Isabelle.Vandernoot@erasme.ulb.ac.be

Benoit Haerlingen benoit.haerlingen@gmail.com

Achim Trubiroha achim.trubiroha@bfr.bund.de

Pierre Gillotay Pierre.Gillotay@ulb.ac.be

Véronique Janssens verojans@ulb.ac.be

Robert Opitz robert.opitz@charite.de

Sabine Costagliola scostag@ulb.ac.be

Correspondence and requests for materials should be addressed to:

Sabine Costagliola (scostag@ulb.ac.be);

IRIBHM, Université Libre de Bruxelles, Campus Erasme, Bat. C., 808 route de Lennik, B-1070 Brussels, Belgium.

Robert Opitz (robert.opitz@charite.de);

Institute of Experimental Pediatric Endocrinology, Charité Universitätsmedizin Berlin, Augustenburger Platz 1, 13353, Berlin, Germany.

1 **Abstract**

2 **Background:** Congenital hypothyroidism (CH) due to thyroid dysgenesis is a frequent
3 congenital endocrine disorder for which the molecular mechanisms remain unresolved in the
4 far majority of cases. This situation reflects in part our still limited knowledge about the
5 mechanisms involved in the early steps of thyroid specification from the endoderm, in
6 particular the extrinsic signaling cues that regulate foregut endoderm patterning. In this study,
7 we used small molecules and genetic zebrafish models to characterize the role of various
8 signaling pathways in thyroid specification.

9 **Methods:** We treated zebrafish embryos during different developmental periods with small
10 molecule compounds known to modulate the activity of Wnt signaling pathway and observed
11 effects in thyroid, endoderm and cardiovascular development using whole mount *in situ*
12 hybridization and transgenic fluorescent reporter models. We used an antisense morpholino
13 to create a zebrafish acardiac model. For thyroid rescue experiments, BMP pathway induction
14 in zebrafish embryos was obtained by using heatshock inducible transgenic lines.

15 **Results:** Interestingly, combined analyses of thyroid and cardiovascular development revealed
16 that overactivation of Wnt signaling during early development leads to impaired thyroid
17 specification concurrent with severe defects in the cardiac specification. When using a model
18 of morpholino-induced blockage of cardiomyocyte differentiation, a similar correlation was
19 observed, suggesting that defective signaling between cardiac mesoderm and endodermal
20 thyroid precursors contributes to thyroid specification impairment. Rescue experiments
21 through transient overactivation of BMP signaling could partially restore thyroid specification
22 in models with defective cardiac development.

23 **Conclusion:** Collectively, our results indicate that BMP signaling is critically required for
24 thyroid cell specification and identify cardiac mesoderm as a likely source of BMP signals.

25

26 **Introduction**

27 The thyroid is an endoderm-derived gland developing from the most anterior part of
28 the gut tube. The thyroid organogenesis starts with the specification of its anlage, a group of
29 thyroid precursor cells that are characterized by co-expression of a unique combination of
30 transcription factors comprising NKX2-1, PAX8, FOXE1, and HHEX (1).

31 The median anlage develops into a diverticulum that evaginates and loses contact with
32 the ventral foregut endoderm to relocate deeper into the subpharyngeal mesenchyme.
33 Terminal differentiation, which leads to functional follicle formation, is initiated during the
34 migration of the thyroid primordium (2).

35 Congenital hypothyroidism (CH) is the most frequent congenital endocrine disorder,
36 affecting approximately one of 2500 in human newborns (3). CH is characterized by reduced
37 serum thyroid hormone levels at birth. It is caused in 85% of the cases by thyroid dysgenesis
38 (TD due to ectopy, athyreosis, or hypoplasia, resulting from an aberration of the thyroid gland
39 embryological development. The molecular mechanisms leading to TD are mostly unknown,
40 with mutations in the known thyroid transcription factors explain only 5% of TD cases (1). It
41 probably reflects our limited knowledge about intrinsic factors and external signals
42 coordinating thyroid organogenesis and suggests that unknown genetic and/or epigenetic
43 factors might be crucial for thyroid development (4).

44 Zebrafish is a valuable model system that has already helped us to improve further our
45 understanding of morphogenetic processes and gene networks involved in thyroid
46 organogenesis (5). Over the past two decades, zebrafish has gained much attention as a
47 genetically tractable vertebrate model to study organogenesis (6). Embryos' optical clarity
48 allows direct visualization of developmental processes and their pathological deviations.
49 Small size, high fecundity, external fertilization, rapid development, and short generation time
50 are important attributes underscoring the utility of zebrafish study of early developmental

51 processes. The value of zebrafish for studies on thyroid development is supported by the fact
52 that several aspects of thyroid morphogenesis are well conserved between zebrafish and
53 mammals (7), (8). Early morphogenetic events, such as thyroid specification, budding, and
54 relocalization into the subpharyngeal mesenchyme, show many similarities in fish and mouse
55 (reviewed in ref. (9)). Moreover, the developing thyroid expresses a similar, but not identical,
56 set of transcription factors in mouse (*NKX2-1*, *PAX8*, *HHEX*, *FOXE1* (1)) and zebrafish
57 (*nkx2.4b* (10), *pax2a*, *pax8*, *foxe1*, *hhex* (7), (10)) embryos. Invalidation of the known thyroid
58 transcription factors in mice leads to athyreosis (*NKX2-1*, *PAX8*, *FOXE1*, *HHEX*) or thyroid
59 ectopy (*FOXE1*) (11). Zebrafish with loss-of-function of *nkx2.4b*, *pax2a*, and *hhex* similarly
60 display athyreosis (7), (9), (12). However, differences exist in the timing of specific
61 morphogenetic events and the anatomy of the mature thyroid tissue. Indeed, although thyroid
62 follicles are encapsulated in a compact organ in mouse, thyroid follicles are loosely scattered
63 along the pharyngeal midline in zebrafish.

64 In this study, we mainly focused on molecular mechanisms that govern the first steps
65 of thyroid specification. At present, the signals that trigger the specification of pharyngeal
66 endodermal cells into thyroid precursors remains unknown. Recent studies demonstrate that
67 tissue-tissue interactions, in particular with the cardiac mesoderm and pharyngeal blood
68 vessels, are essential for correct thyroid development (13), (5). Defective pharyngeal vessel
69 development has been shown to cause thyroid anomalies in mice and zebrafish (14), (15).
70 There are also pieces of evidence coming from human disease studies since an increased
71 prevalence of congenital cardiovascular anomalies is observed in patients with thyroid
72 dysgenesis compared to the healthy population (16). However, the mechanisms underlying
73 tissue-tissue interactions during thyroid development (particularly between the developing
74 thyroid and the cardiac mesoderm and pharyngeal vessels) and the signals involved in this
75 crosstalk are poorly understood. While a crucial role of FGF expression in the mesoderm

76 surrounding the developing thyroid has been demonstrated in mouse and zebrafish (17), (18),
77 the potential functions of other major signaling pathways in thyroid organogenesis is still to
78 be clarified (2), (19). A significant advantage of the zebrafish model in cardiovascular
79 development studies is that zebrafish embryos and larvae can survive for several days without
80 a functional heart or in the absence of blood circulation (20). This facilitates the
81 characterization of developmental effects over an extended developmental period, compared
82 to most mouse models with cardiovascular defects.

83 To improve our understanding of the role of extrinsic signaling cues in thyroid
84 development, we recently exploited the amenability of zebrafish embryos for small molecule
85 screenings to identify candidate signaling pathways (12), (21). From a literature review, we
86 first identified a collection of small molecules known to interfere with common signaling
87 pathways in zebrafish. The pharmacological screening readily identified modulators of Wnt,
88 BMP, FGF, and TGF- β signaling to cause distinct effect patterns of disturbed thyroid
89 organogenesis (e.g., agenesis, hypoplasia, ectopy) (21). In this paper, we focused on the
90 phenotypic description, using thyroid and cardiovascular markers, of early thyroid
91 development after Wnt modulation and propose a mechanistic explanation.

92 Wnt signaling pathway is an evolutionarily conserved signal transduction pathway that
93 regulates crucial aspects of cell fate determination, cell migration, cell polarity and cell
94 differentiation during embryonic development (22). Wnt proteins are secreted glycoproteins
95 that bind to the N-terminal extra-cellular cysteine-rich domain of the Frizzled (Fz) receptor
96 family, interacting with the LRP5/6 co-receptors. To date, several intracellular signaling
97 branches/cascades downstream of the Fz receptors have been identified including a canonical
98 (β -catenin dependent) pathway and a non-canonical (β -catenin-independent) pathway. Some
99 Wnt ligands act preferentially on one pathway or the other, but the activated pathway mostly
100 depends on the cellular context. Without Wnt canonical signaling activation, cytoplasmic β -

101 catenin is degraded by a β -catenin destruction complex, which includes Axin, adenomatosis
102 polyposis coli (APC), protein phosphatase 2A, glycogen synthase kinase 3 (GSK3) and
103 casein kinase 1 α (CK1). Binding of a Wnt ligand to its receptor leads to a series of events
104 that disrupt the β -catenin destruction complex, which is required for the β -catenin
105 translocation into the nucleus and activation of target genes (23), (24).

106 The functions of Wnt/ β -catenin signaling in embryogenesis have been extensively
107 studied in different animal models. It plays a crucial biphasic role in heart development, as
108 demonstrated in *in vitro* cells and zebrafish: in pregastrula stages, canonical Wnt promotes the
109 specification of the precardiac mesoderm into cardiomyocyte progenitors, but it inhibits the
110 cardiac differentiation of these cells during gastrula stages (25), (26). It has already been
111 demonstrated that this pathway also plays a very important role in the specification and
112 development of endoderm-derived organs, like liver and pancreas. An anterior-posterior
113 gradient of Wnt activity in *Xenopus* plays a crucial role in endodermal patterning, the anterior
114 endoderm giving rise among others to liver, lung, and thyroid, the posterior endoderm leading
115 to intestinal fate (27). At later stages in zebrafish, Poulain *et al.* have shown that Wnt pathway
116 is necessary for liver progenitors proliferation (28). However, very little data exist on the role
117 of Wnt in thyroid development and/or maintenance.

118 Therefore, this study aims to examine the effects of the canonical Wnt signaling
119 pathway on thyroid development in zebrafish, in regard to the adjacent cardiogenesis. We
120 used different chemicals and genetic models to modulate canonical Wnt signaling during
121 gastrula and early somitogenesis stages and observed effects of such modulation on thyroid
122 organogenesis. We succeeded to partially rescue thyroid defects obtained after Wnt activation
123 when combining this chemical treatment with induction of BMP pathway using heatshock
124 inducible transgenic lines.

125

126 **Material and methods**

127 *Zebrafish husbandry and embryo culture*

128 Zebrafish (*Danio rerio*) embryos were obtained from natural spawning of adult fish, raised at
129 28.5°C according to Westerfield (29) and staged in hours postfertilization (hpf) as described
130 by Kimmel *et al.* (30) In addition to wild-type (31) and *casper* mutant lines (32), different
131 transgenic lines were used in this study: *Tg(tg:mCherry)* (5), *Tg(kdrl:EGFP)* (33),
132 *Tg(myf7:EGFP)* (34), *Tg(7xTCF-Xla.Siam:GFP)ia4* (35), *Tg(sox17:EGFP)* (36),
133 *Tg(hsp70l:bmp2b)* (37) and *Tg(hsp70l:wnt8a-EGFP)* (38). Embryos were dechorionated at 24
134 hpf using 0.6 mg/mL pronase (Sigma), anesthetized in 0.016% tricaine (Sigma), fixed in 4%
135 phosphate-buffered paraformaldehyde (PFA; Sigma) overnight at 4°C, washed in PBS
136 containing 0.1% Tween 20 (PBST), gradually transferred to 100% methanol, and stored at
137 -20°C until used for *in situ* hybridization or immunofluorescence analyses. If indicated,
138 pigmentation of embryos was inhibited by adding 0.003% 1-phenyl-2-thiourea (PTU; Sigma)
139 (39) to the embryo medium at 24 hpf. All zebrafish work at the Institute of Interdisciplinary
140 Research in Molecular Human Biology followed protocols approved by the Institutional
141 Animal Care and Use Committee.

142

143 *Small molecule treatment*

144 We used timed embryo treatment with BIO (Sigma, B1686), 1-Azakenpaullone
145 [AZA] (Sigma, A3734), and IWR-1 (Sigma, I0161) to modulate the canonical Wnt signaling
146 pathway during distinct developmental periods. BIO and AZA act as canonical Wnt activators
147 due to GSK3 β inhibition (40). In contrast, IWR-1 stabilizes the destruction complex, thereby
148 acting as an inhibitor of Wnt signaling (41). Stock solutions of BIO (5 mM), AZA (5 mM),
149 and IWR-1 (10 mM) were prepared in dimethyl sulfoxide (DMSO). Test solutions were

150 prepared by diluting the stock solutions in embryo medium. A control treatment containing
151 0,1% DMSO was used in all experiments involving a drug treatment.

152

153 *Heat-shock treatments*

154 Timed global overactivation of Wnt and BMP signaling was induced by heat-shock treatment
155 of the progeny from matings of WT fish with heterozygous *Tg(hsp70l:wnt8a-GFP)* (38) or
156 *Tg(hsp70l:bmp2b)* (37) fish, respectively. Embryos obtained from these matings were raised
157 under standard conditions until heat-shock to induce global overexpression of EGFP-tagged
158 Wnt8a or Bmp2b. For the heat-shock treatments, embryos were transferred to dishes
159 containing prewarmed embryo medium at 40°C and incubated in an incubator for 30 min at
160 40°C. After heat-shock treatment, embryos were transferred to Petri dishes containing fresh
161 medium and allowed to develop further at 28.5°C under standard conditions. Carriers of the
162 *hsp70l:wnt8a-EGFP* transgene were identified 3 hours after heat-shock by means of their
163 EGFP expression. Embryos carrying the *hsp70l:bmp2b* transgene were identified by their
164 dorsalized phenotype if heat-shocked at early somitogenesis or by PCR genotyping if
165 embryos were heat-shocked at later stages (15 or 20 hpf). For the latter, PCR genotyping was
166 performed after completion of WISH experiments as previously described (42) using the
167 following primers: Forward 5'-CATGTGGACTGCCTATGTTTCATC-3' (primer located in
168 *hsp70l* promoter sequence); Reverse 5'-GAGAGCGCGGACCACGGCGAC-3' (primer
169 located in *bmp2b* coding sequence).

170

171 *Whole-mount in situ hybridization (WISH)*

172 DNA templates for synthesis of *nkx2.4b*, *tg*, *nkx2.5*, *egfp*, *mef2cb*, *gata4*, *gata5*, *hhex*,
173 *foxa2*, *foxa3*, *pdx1*, *prox1*, and *bmp4* riboprobes were generated by PCR (see **Supplemental**
174 **Table 1** for primer sequences). Plasmids for *amhc*, *vmhc*, *myl7*, *scl*, and *hand2* riboprobes

175 have been used as described (43), (44), (45). Single-color WISH using digoxigenin (DIG)-
176 labeled riboprobes and anti-DIG antibody conjugated to alkaline phosphatase was performed
177 essentially as described in Thisse and Thisse (46) and Opitz *et al* (5). Riboprobe hybridization
178 was performed at 65°C overnight, and probes were detected using an anti-DIG antibody
179 (1:6000; Roche). Staining reactions were performed with the alkaline phosphatase substrates
180 BM Purple (Roche) or NBT/BCIP (Roche). For dual-color WISH, riboprobes labeled with
181 DIG, dinitrophenol (DNP), or fluorescein (FLU) were used, and sequential alkaline
182 phosphatase staining was performed with BM Purple and Fast Red (Sigma) as described
183 (21). We first detect the DIG or DNP riboprobes with anti-DIG or anti-DNP antibody using
184 BM Purple (for most genes) or NBT/BCIP (for *tg*) staining solution and used an anti-FLU
185 antibody in combination with FastRed for detection of the FLU probe in a second step.
186 Removal of the antibodies after the first staining step was performed by 2x 5 min incubation
187 in 100 mM glycine-HCl (pH 2.2).

188 Fluorescent WISH (FISH) using a DIG-labeled riboprobe for *nkx2.4b* was performed as
189 described (5). Antibodies used in WISH and FISH experiments are listed in **Supplemental**
190 **Table 2**. Stained embryos were washed in PBST, postfixed in 4% PFA and embedded in 90%
191 glycerol for whole-mount imaging or in 7% low melting point agarose (Lonza) for vibratome
192 sectioning. Whole-mount images of WISH and FISH were acquired using a MZ16F Leica
193 stereomicroscope equipped with a DFC420C camera or a Leica microscope DMI6000B
194 equipped with a DFC365FX camera, respectively. Vibratome tissue sections at 50–60µm
195 thickness were cut on a Leica VT1000S vibratome and mounted in Glycergel (Dako).
196 Confocal images of vibratome sections were acquired using an LSM510 confocal microscope
197 (Zeiss).

198

199 *Whole-mount immunofluorescence (WIF)*

200 WIF was performed essentially as described (47). Briefly, after rehydration into
201 PBST, embryos were immersed in blocking buffer (PBST containing 1.0% DMSO, 1%
202 bovine serum albumin [BSA], 5% horse serum, and 0.8% Triton X-100) for 2 h. Embryos
203 were then incubated overnight in blocking buffer containing primary antibodies at 4°C. After
204 several washing steps in PBST containing 1% BSA, embryos were incubated with secondary
205 antibodies overnight at 4°C. Specifications and sources of primary and secondary antibodies
206 used to detect EFGP green fluorescent protein (48) and pSMAD1/5/8 protein in zebrafish
207 embryos are provided in **Supplemental Table 2**. Stained embryos were washed in PBST and
208 embedded in 90% glycerol for fluorescence microscopy. Images were acquired with a Leica
209 DFC365FX camera mounted on a Leica DMI6000B. Combined FISH and WIF staining was
210 performed as described (5). Confocal images were acquired using a LSM510 confocal
211 microscope (Zeiss).

212

213 *RNA extraction and RT-qPCR*

214 For total RNA preparation, pools of 10-20 embryos per sample were lysed in RNeasy
215 Lysis buffer (Qiagen) containing 1% 2-mercaptoethanol (Sigma). Total RNA was isolated
216 using RNeasy RNA preparation microkit (Qiagen) according to the manufacturer's
217 instructions, including on-column treatment with DNase I (Qiagen). Reverse transcription
218 was done using Superscript II kit (Invitrogen). Reverse transcription quantitative PCR (RT-
219 qPCR) was performed in duplicate using Kapa SYBR Fast (KapaBiosystems) mix and a CFX
220 Connect Real-Time PCR System (Biorad).

221 Relative values for target transcript abundance in individual samples were determined by the
222 comparative C_T method ($\Delta\Delta C_T$) according to Pfaffl *et al.* (2001) (49), and data are presented
223 as relative expression values normalized to the reference gene *rpl13* (NM_212784.1) whose
224 expression remained constant upon treatment. Primers used were as follows: *rpl13*, forward

225 TCTGGAGGACTGTAAGAGGTATGC, reverse AGACGCACAATCTTGAGAGCAG (50);
226 *egfp*, forward AGAACGGCATCAAGGTGAAC, reverse TGCTCAGGTAGTGGTTGTCG.
227 Gene expression profile was confirmed in triplicate (3 different batches of embryos). Data
228 were expressed as mean \pm SD. Pairwise comparisons were performed using the Student *t*-test.
229

230 *Fluorescence-activated cell sorting*

231 Cell suspensions were prepared from *Tg(sox17:EGFP)* transgenic embryos at 30
232 hpf. Embryos were digested in HBSS (Gibco) containing 0.25% trypsin (Gibco) and 2 mM
233 EDTA (Invitrogen). Single-cell solutions were obtained by constant pipetting. Reaction was
234 stopped by adding CaCl₂ (final concentration: 1 mM) and FBS (final concentration: 10%).
235 Cells were pelleted by centrifugation and washed with PBS containing 0.4% BSA and 2 mM
236 EDTA. Finally, resuspended cells were passed through a 40 μ M nylon mesh (Falcon) into a
237 FACS tube (Falcon) and the GFP⁺ fractions were analyzed by a fluorescent-activated cell
238 sorter (FACS Aria: FACSDiva Software (BD)). About 50 embryos were sampled per
239 condition, and each experiment was performed in triplicate.

240

241 *Morpholino microinjection*

242 For inhibition of the *mef2ca* and *mef2cb* transcripts, zebrafish embryos were injected
243 with morpholino (MO) antisense oligonucleotides that have previously been validated for
244 their knockdown specificity and efficacy (51), (52). 3nL (2ng/nL) of a translation-blocking
245 *mef2d/c*-MO (tb-MO; 5'-ATGGGGAGGAAAAAGATCCAGATTC-3') was injected as
246 previously described (51). Working solutions of MOs were prepared in 0.12 M KCl
247 containing phenol red, and 3 nL were microinjected into the yolk of one- to two-cell stage
248 embryos. Non-injected embryos served as control embryos.

249

250 *Statistics*

251 For the statistical analyses of thyroid and cardiac phenotypes in the rescue
252 experiments, Fisher tests were conducted using the software package GraphPad Prism 4.0
253 (GraphPad, San Diego, CA). Differences were considered significant at $p < 0,05$.

254

255 **Results**

256 *Drug-induced manipulation of canonical Wnt signaling disrupts early thyroid development*

257 We recently performed a small molecule screen to identify signaling pathways
258 involved in early zebrafish thyroid development (21). In these experiments, pharmacological
259 manipulations of canonical Wnt signaling during gastrula stage resulted in abnormal thyroid
260 marker expression, and most notably, in a severe reduction of *nkx2.4b* expression at thyroid
261 anlage stages (28 hpf) following overactivation of Wnt signaling.

262 To characterize in more detail the thyroidal effects resulting from enhanced Wnt
263 signaling, we performed additional treatment experiments with BIO and AZA, two drugs
264 known to activate Wnt/ β -catenin signaling (40). Consistent with our previous results,
265 treatment of zebrafish embryos with BIO or AZA during the gastrulation period (6 to 10 hpf)
266 caused concentration-dependent decreases of *nkx2.4b* expression in 28 hpf embryos (**Figure**
267 **1**). Maximal effects on thyroidal *nkx2.4b* expression (i.e. complete absence of a detectable
268 WISH staining) were evident at 5 μ M BIO and 5 μ M AZA. In addition to the marked effects
269 on the thyroidal *nkx2.4b* expression domain, BIO and AZA treatments also caused
270 concentration-dependent decreases in the size of the *nkx2.4b* expression domain in the
271 forebrain. The drug-induced effects on forebrain *nkx2.4b* expression correlated closely with
272 other visible signs of global posteriorization, including loss of anterior neural tissue and
273 reduced size or absence of the eyes (53), (54). Although we did not quantify the relative size
274 reductions of thyroidal and forebrain *nkx2.4b* expression domains in 28 hpf embryos

275 following different BIO and AZA treatments, we noted a similar sensitivity to drug treatment
276 for both expression domains when embryos were treated between 6 – 10 hpf.

277 Concentration-dependent effects on thyroid development were also evident when BIO-
278 and AZA-treated embryos were analyzed for thyroid marker expression at 55 hpf (**Figure 2**).
279 WISH analysis of *nkx2.4b* expression revealed concurrent reductions in the size of thyroidal
280 and forebrain expression domains in treated embryos. Moreover, BIO and AZA treatment
281 strongly reduced the expression of the functional thyroid differentiation marker, thyroglobulin
282 (*tg*), in 55 hpf embryos. However, we also noted that the majority of 55 hpf embryos treated
283 with high drug concentrations during gastrula stages displayed at least some residual staining
284 for *nkx2.4b* and *tg* despite undetectable thyroid marker expression at the thyroid anlage stage
285 (28 hpf). This was observed in all experiments involving drug treatment from 6 to 10 hpf.

286 Conversely, treatment of gastrulating embryos with 10 μ M IWR-1, a small molecule
287 inhibitor of canonical Wnt signaling, resulted in additional ectopic domains of thyroidal
288 *nkx2.4b* and *tg* expression (**Supplementary figure 1**). In 28 hpf embryos, the additional
289 ectopic *nkx2.4b* expression was detected posterior to the orthotopic thyroidal *nkx2.4b*
290 expression domain, whereas in 55 hpf embryos, supernumerary clusters of *tg* expression were
291 detectable at irregular posterior positions. Taken together, these data indicate that the
292 canonical Wnt pathway negatively regulates thyroid specification during gastrulation stage in
293 zebrafish as drug-mediated activation or inhibition of Wnt activity during gastrulation impairs
294 or amplifies thyroid specification, respectively.

295

296 *Small molecule compounds rapidly act on Wnt signaling*

297 We next took advantage of an available Wnt signaling biosensor line, *Tg(7xTCF-*
298 *Xla.Siam:GFP)^{ia4}*, to verify that the small molecule compounds BIO, AZA and IWR-1
299 effectively alter canonical Wnt signaling activities within a short space of time under the

300 experimental conditions that resulted in irregular thyroid development. For this purpose, we
301 treated *Tg(7xTCF-Xla.Siam:GFP)^{ia4}* embryos with BIO (5 μ M), AZA (5 μ M) or IWR-1 (10
302 μ M) from 6 to 10 hpf and monitored the expression of *GFP* mRNA during the course of drug
303 treatment by WISH and RT-qPCR (**Supplementary figure 2**).

304 WISH analyses of *GFP* mRNA expression in BIO- and AZA-treated embryos showed
305 a rapid and robust up-regulation of *GFP* mRNA expression when compared to DMSO-treated
306 embryos (0.1% DMSO) indicating effective overactivation of canonical Wnt signaling in
307 drugged embryos within 2 hours after the beginning of drug treatment. Consistently, IWR-1
308 treatment resulted in reduced *GFP* mRNA expression, evident within 2-3 hours after the
309 beginning of drug treatment. Although several embryos treated with these small molecule
310 compounds experienced slight developmental delay, the drug-induced alterations in reporter
311 expression were robustly detectable in comparison with vehicle control embryos. In further
312 experiments, we also corroborated the effects of BIO treatment on *GFP* mRNA expression by
313 RT-qPCR. As shown in **Supplementary figure 2**, treatment of *Tg(7xTCF-Xla.Siam:GFP)^{ia4}*
314 embryos with 5 μ M BIO resulted in 2.5- to 3-fold increases of whole embryo expression
315 levels of *GFP* mRNA within 2 hours after initiation of BIO treatment. Together, these data
316 demonstrate that, under our experimental conditions, the drug treatments faithfully altered
317 canonical Wnt signaling.

318

319 In order to provide an independent line of evidence that defective thyroid development
320 is due to transient overactivation of Wnt/ β -catenin signaling during gastrulation, we
321 manipulated Wnt/ β -catenin signaling by heat-shock-induced overexpression of *wnt8a* in
322 *Tg(hsp70l:wnt8a-GFP)* embryos (38). *Wnt8a* specifically activates Wnt/ β -catenin signaling in
323 zebrafish embryos and a 30 min heat-shock of transgenic *Tg(hsp70l:wnt8a-GFP)* embryos at
324 6 hpf resulted in a marked neural posteriorization phenotype and disturbed early thyroid

325 development (**Figure 3**). Non-transgenic embryos showed no discernible phenotypes in
326 response to the heat-shock treatment. The thyroid phenotype caused by transient *wnt8a*
327 overexpression in the genetic model closely resembled the phenotypes observed following
328 treatment with 4-5 μ M BIO or AZA. Specifically, our WISH analyses failed to detect *nkx2.4b*
329 expression in the thyroid anlage region of heat-shocked embryos carrying the *wnt8a-GFP*
330 transgene at 28 hpf and a detectable, though strongly diminished, *tg* expression in 55 hpf
331 transgenic embryos (**Figure 3**). Taken together, these experiments verified that the selected
332 drug concentrations cause overactivation of Wnt/ β -catenin signaling and that enhanced
333 Wnt/ β -catenin signaling during gastrula stages leads to defects in thyroid development.

334

335 *Effects of early Wnt overactivation on endoderm development*

336 Our initial experiments with BIO and AZA showed that treatment with different drug
337 concentrations during gastrulation causes thyroid abnormalities and a strong posteriorization
338 of neural ectoderm. Considering that the latter phenotype is a well-characterized effect of
339 enhanced Wnt signaling during early development (55), we next examined whether
340 endodermal development is similarly affected by a global posteriorization activity due to
341 enhanced Wnt signaling and might thus explain the loss of thyroid marker expression in the
342 anterior endoderm.

343 To address this question, we first treated embryos of the transgenic *Tg(sox17:EGFP)*
344 line with BIO (5 μ M) or AZA (5 μ M) between 6 – 10 hpf and analyzed the gross
345 morphology of their foregut endoderm at different embryonic stages, in comparison to that of
346 DMSO-treated embryos. While a neural posteriorization phenotype (loss of anterior neural
347 tissue) was readily detectable in BIO- and AZA-treated *Tg(sox17:EGFP)* embryos, the gross
348 morphology of the anterior endoderm appeared unaffected in these embryos
349 (**Supplementary figure 3**). In addition, we used FACS to compare the number of GFP+ cells

350 in 30 hpf *Tg(sox17:EGFP)* embryos following treatment with DMSO (0.1%) and BIO
351 (5 μ M) but did not detect a decrease in the number of GFP+ cells in BIO-treated embryos
352 (**Supplementary figure 3**). Thus, in contrast to the overt effects on anterior neural tissue
353 development, no visible dysgenesis of the anterior endoderm was detected in
354 *Tg(sox17:EGFP)* following early Wnt overactivation.

355 To further study possible global endodermal patterning defects in BIO and AZA-
356 treated embryos, we analyzed the expression of a panel of informative endodermal marker
357 genes by WISH (**Figure 4**). We first confirmed that thyroidal expression of *nkx2.4b* and *hhex*
358 is affected similarly by BIO and AZA treatment (see **Figure 4A-D**). In addition to the
359 thyroid, *hhex* is expressed in the developing liver and pancreas. Interestingly, *hhex* expression
360 was selectively repressed in the thyroid anlage of BIO-treated embryos and was maintained in
361 the liver/pancreas region (**Figure 4D**). Notably, the shape and position of the hepatic and
362 pancreatic *hhex* expression domains were altered in BIO-treated embryos. Therefore, we
363 analyzed the expression of *foxa2*, a master regulator of foregut endoderm patterning. Notably,
364 our WISH analyses did not reveal gross changes in the *foxa2* anterior-posterior expression
365 pattern following BIO treatment (**Figure 4E,F**). However, when analyzing *foxa3* expression,
366 a key regulator of posterior endoderm development, we noted that its expression domain
367 appeared extended more anteriorly in many embryos after BIO treatment (**Figure 4G,H**).
368 Analyses of *pdx1* and *prox1a* expression confirmed that hepatic and pancreatic markers are
369 unaffected in BIO-treated embryos and that diminished expression in response to canonical
370 Wnt overactivation is limited to thyroidal marker genes (**Figure 4I-L**).

371 Collectively, our analyses indicate that the loss of thyroid marker expression caused
372 by overactivation of canonical Wnt signaling during gastrulation is not due to a general defect
373 in anterior foregut formation. However, as indicated by the irregular anterior *foxa3* expression
374 in BIO-treated embryos and the posterior extension of thyroid marker expression in IWR-1-

375 treated embryos, we cannot rule out that a Wnt-induced foregut endoderm posteriorisation
376 might contribute to the thyroid defects seen in the most anterior part of the foregut.

377

378 *Cardiac phenotype is correlated with thyroid phenotype after gastrula Wnt activation*

379 A recurrent theme in the development of endoderm-derived organs is the critical role
380 of tissue-tissue interactions, particularly between the endoderm and adjacent mesodermal
381 tissues (56), (28). Observations made during our initial small molecule screening experiments
382 (21) indicated that overactive Wnt signaling might induce the concurrent cardiac and
383 thyroidal maldevelopment. To examine this possible relationship in more detail, we first
384 confirmed that drug-induced overactivation of Wnt signaling during gastrula stages results in
385 a severe inhibition of heart formation (**Supplementary figure 4**) as previously reported for
386 genetic models with overactivation of canonical Wnt signaling (26), (25). When treated
387 between 6 to 10 hpf, effects of Wnt-activating drugs on heart development appeared
388 concentration-dependent, and we noticed that development of ventricular cardiomyocytes was
389 more severely affected, compared to that of atrial cardiomyocytes (**Supplementary figure**
390 **4**). Notably, the concentrations at which BIO and AZA caused severe cardiac
391 maldevelopment (**Figure 5**) overlapped the range at which repression of thyroid markers was
392 detected.

393

394 To characterize the evolution of the cardiac differentiation defects in drugged
395 embryos, we examined the expression of various cardiac differentiation markers at earlier
396 stages of cardiac development (**Figure 5**). Comparative WISH analyses of BIO- and DMSO-
397 treated embryos showed severely reduced expression of transcription factors regulating
398 cardiovascular development such as *nkx2.5*, *mef2cb*, and *scl* in response to Wnt
399 overactivation. Consistent with previous studies employing genetic zebrafish models (25),

400 expression levels of these genes were dramatically decreased as early as 13 hpf in BIO-treated
401 embryos. Conversely, we observed only mild changes, if any, in the expression of
402 transcription factors with a broader lateral plate mesoderm expression domain, including
403 *gata4*, *gata5*, and *hand2* (**Figure 5**). Given that endodermal progenitors of the thyroid
404 lineage develop in close vicinity to the anterior lateral plate mesoderm containing cardiac
405 precursors zebrafish (17), we hypothesized that diminished availability of cardiac mesoderm-
406 borne signaling cues contributes to the defective thyroid development in BIO-treated
407 embryos.

408

409 To evaluate a possible causal relationship between inhibited cardiac development and
410 thyroid dysgenesis, we examined the co-occurrence of cardiac and thyroid developmental
411 defects over a range of drug concentrations by dual-color WISH of cardiac (*myl7*) and
412 thyroid (*nkx2.4b*) marker expression in 28 hpf embryos (**Figure 6**). For embryos treated with
413 increasing concentrations of BIO from 6 to 10 hpf, we observed a gradual loss of
414 cardiomyocytes correlated with a gradual reduction in thyroid marker expression (**Figure**
415 **6A-F**). Notably, although we observed embryos without any detectable thyroidal *nkx2.4b*
416 expression but still displaying remnant *myl7* positive cardiac tissue, we never observed any
417 embryo with detectable thyroid marker expression in the complete absence of *myl7* cardiac
418 expression. While these observations are compatible with the hypothesis that the availability
419 of cardiac mesoderm and associated signaling cues are prerequisites for thyroid lineage
420 specification to occur, the concurrent global posteriorization phenotype of the embryos
421 prevented us from distinguishing the relative impact of cardiac dysgenesis against a possible
422 posteriorized patterning in the etiology of the thyroid specification defect.

423 It has been demonstrated that the later the embryos are treated with Wnt activators
424 during gastrulation, the weaker is the posteriorization effect. Still, cardiac development

425 remains highly sensitive to these later treatments (25). Therefore, we progressively shifted the
426 treatment periods towards later stages and assessed the impact of drug-induced Wnt signaling
427 on global posterization and cardiac and thyroid development in these embryos. As expected,
428 gross morphological signs of posterization were greatly reduced if embryos were treated from
429 9 to 12 hpf (**Figure 6G-L**). However, Wnt overactivation at these later stages caused still a
430 severe inhibition of cardiac development. Moreover, It appeared that the prevalence and
431 severity of cardiac dysgenesis and thyroid misspecification correlated closely in embryos
432 treated with Wnt-activating drugs between 9 and 12 hpf. We made the same observations
433 when we treated the embryos from 10 to 13 hpf or from 9 to 24 hpf (**Figure 7**). However, we
434 noted that initiation of drug treatment at 11 hpf or later stages caused progressively milder
435 effects on both cardiac and thyroid differentiation as assessed by WISH for cardiac *myl7*
436 expression and thyroidal *nkx2.4b* expression (**Figure 7I,J**).

437

438 *Experimental depletion of cardiomyocyte developmental is associated with thyroid dysgenesis*

439 To further examine the hypothesis that depletion of cardiac mesoderm results in a
440 failure of thyroid cell specification, we sought for cardiac differentiation-defective zebrafish
441 models. To the best of our knowledge, a zebrafish model completely lacking cardiac cells
442 while maintaining normal anterior endoderm has not yet been described. Hinitz *et al.* recently
443 described a severe deficiency in cardiomyocyte differentiation in a dual loss-of-function
444 model for zebrafish cardiac transcription factors *mef2ca* and *mef2cb* (51), (52). For our study,
445 we used an antisense morpholino (*mef2c/d*-MO) developed by the same group that reportedly
446 ablates several Mef2 proteins and faithfully replicates the cardiac phenotype present in
447 *mef2ca/mef2cb* double mutant fish (52). In our hands, injection of the *mef2c/d*-MO into wild-
448 type embryos, hereafter called Mef2c-deficient embryos, robustly inhibited cardiomyocyte
449 development as evident from only faint *myl7* staining of small and very thin heart tube

450 remnants at 28 and 55 hpf (**Figure 8**). Compared to control embryos, we also observed a
451 greatly reduced expression of *nkx2.4b* in the thyroid anlage of 28 hpf *mef2c/d*-morphant
452 embryos (**Figure 8A-D**). Across several *mef2c/d*-MO injection experiments, we observed
453 that prevalence and severity of cardiac malformation correlated with the extent of impaired
454 thyroid marker expression in 28 hpf morphant embryos. Detectable domains of *nkx2.4b*
455 expression displayed a weaker staining intensity and were of a smaller size in *Mef2c*-deficient
456 embryos relative to control embryos. Comparison of control and *Mef2c*-deficient embryos at
457 55 hpf revealed an irregular organization of *tg*-expressing cells in *Mef2c*-deficient embryos,
458 which displayed a fainter *tg* staining of individual cells. Collectively, observations made in
459 this *Mef2c*-deficient zebrafish model of impaired cardiomyocyte differentiation support the
460 contention that thyroid anlage specification relies on normal cardiac development.

461

462 *Enhancing BMP signaling causes partial rescue of thyroid defects in BIO-treated embryos*

463 Cardiac mesoderm expresses a number of diffusible growth factors, including several
464 FGF and BMP ligands (17), (52) with potential thyroid specification-inducing capacity (17),
465 (57), (58). In this respect, our recent small molecule screening showed that pharmacological
466 inhibition of either FGF or BMP signaling during somitogenesis causes a failure of thyroid
467 anlage formation in zebrafish (21). Thus, we reasoned that reduced availability of cardiac-
468 borne signaling cues might explain the defective thyroid anlage formation observed in our
469 experimental models (*Wnt* overaction, *mef2c/d*-morphants) displaying perturbed cardiac
470 development in this study.

471 To address the question that diminished BMP signaling might contribute to thyroid
472 phenotypes observed in embryos with after *Wnt* overactivation, we first examined
473 endogenous *bmp4* expression in control embryos and embryos treated with BIO from 6 to 10
474 hpf. WISH analyses of 26 hpf embryos showed that the *bmp4* expression of cardiac tissue

475 adjacent to the thyroid anlage region in normally developing embryos (**Supplementary**
476 **figure 5A**) is completely ablated in BIO-treated embryos (**Supplementary figure 5B**).
477 Similarly, Hinitz *et al.* reported that Mef2c-deficient embryos lack *bmp4* expression in the
478 cardiac region (52). In normally developing 42 hpf embryos, we also observed that cells
479 contained in the forming thyroid bud display enhanced BMP signaling compared to adjacent
480 foregut tissue (**Supplementary figure 5C-E**).

481 Next, we used a heat shock-inducible system to globally enhance BMP signaling
482 during somitogenesis stages and assessed the effects of ectopically induced BMP signaling on
483 thyroid development in control and BIO-treated embryos. For this purpose, we treated
484 embryos from *Tg(hsp70l:bmp2b)* founders with either DMSO (0.1%) or BIO (5 μ M) from 8
485 to 11 hpf and then exposed these embryos to heat-shock treatment at either early
486 somitogenesis (11 hpf), mid-somitogenesis (15 hpf), late somitogenesis (20 hpf) or
487 repeatedly during the course of somitogenesis (at 11, 15, 20 hpf). Subsequent WISH analyses
488 of thyroid and cardiac markers at 28 hpf revealed different phenotypes depending on the
489 pretreatment (DMSO, BIO) and the timing of heat shock-induced *bmp2b* overexpression.

490 Consistent with a proposed role of BMP for thyroid cell specification, global
491 overactivation of BMP signaling in DMSO-treated embryos (controls) resulted in enhanced
492 expression of *nkx2.4b* (**Figure 9A-I**). Not only was *nkx2.4b* staining strongly increased in
493 these embryos, but the majority of affected embryos also showed a dramatic and irregular
494 expansion of thyroid marker expression along the anterior-posterior axis. Concurrently,
495 DMSO-treated embryos, when heat-shocked at early somitogenesis, failed to form a normal
496 heart tube but showed a severely perturbed expression pattern of the cardiac marker *myl7* with
497 bilateral expression domains extending irregularly along the anterior-posterior axis (**Figure**
498 **9C**). When we applied heat-shock on *Tg(hsp70l:bmp2b)* embryos at mid or late somitogenesis
499 stages, we observed that the thyroid anlage and primitive heart tube formed at orthotopic

500 positions (**Figure 9D-G**). We also observed a moderate enlargement of the *nkx2.4b*
501 expression domain in these embryos. Embryos that were repeatedly heat-shocked during
502 somitogenesis showed a phenotype similar to early somitogenesis heat shock (**Figure 9H,I**).
503 Collectively, the timed heat-shock experiments in DMSO-treated embryos showed that the
504 endoderm is competent at all somitogenesis stages to respond to BMP overactivation with an
505 enhanced thyroid marker expression.

506 Heat-shock experiments with embryos pretreated with BIO (5 μ M) from 8-11 hpf
507 showed that global overactivation of BMP signaling could partially rescue the BIO-induced
508 lack of thyroid marker expression at 28 hpf. WISH analyses and subsequent genotyping of
509 stained specimens showed that heat-shock treatment of non-transgenic BIO-treated embryos
510 did not improve *nkx2.4b* expression, irrespective of the timing of heat-shock induction during
511 somitogenesis (**Figure 9J-R**). In stark contrast, BIO-treated embryos carrying the
512 *hsp70l:bmp2b* transgene showed a strong *nkx2.4b* expression in the thyroid region when heat-
513 shock induction of BMP signaling was performed at early somitogenesis (11 hpf) (**Figure**
514 **9K,L**) or when heat-shock was repeatedly applied at 11, 15 and 20 hpf (**Figure 9Q,R**). Just
515 as observed in DMSO-treated embryos (see **Figure 9C**), overactivation of BMP signaling in
516 BIO-treated embryos at early somitogenesis resulted in irregularly shaped and positioned
517 *nkx2.4b* expression domains, often characterized by an elongated shape along the anterior-
518 posterior axis (**Figure 9L**).

519 The capacity of BMP overactivation to rescue thyroid marker expression in BIO-
520 treated embryos decreased markedly at later somitogenesis stages (see **Figure 9N**), and no
521 rescue of *nkx2.4b* expression was detectable for heat-shock treatments carried out at 20 hpf
522 (see **Figure 9P**). Thus, in contrast to DMSO-treated embryos, embryos treated with BIO
523 lacked the competence to enhance thyroidal *nkx2.4b* expression in response to overactivation
524 of BMP signaling at late somitogenesis stages. Accordingly, in this model, enhancing BMP

525 signaling alone at mid- and late somitogenesis stages is not sufficient to rescue thyroid
526 specification defects.

527 One characteristic feature of BIO-treated embryos displaying a rescue in *nkx2.4b*
528 expression following early heat-shock treatment (11 hpf) was the presence of irregular
529 ectopic patches of *myl7*-expressing cells near the *nkx2.4b*-expressing cells. Although we
530 observed variable amounts of *myl7*-expressing cells across individual embryos from all heat-
531 shock treatment groups (see **Figure 9N,P**), it was only in the group of BIO-treated embryos
532 receiving heat-shock treatment at early somitogenesis (11 hpf) that we consistently observed
533 a surplus of *myl7*-expressing cells in the vicinity of *nkx2.4b*-expressing cells. However, we
534 note that we never observed a near full rescue of heart tube formation due to our heat shock
535 treatments in BIO-treated embryos.

536

537 *Enhancing BMP signaling causes partial rescue of thyroid defects in Mef2c-deficient embryos*

538 Given that enhanced BMP signaling could only achieve a rescue of thyroid specification
539 defects in BIO-treated embryos under conditions that concurrently induced a small but
540 consistent cardiac cell differentiation, we next applied a similar rescue approach to *Mef2c*-
541 deficient. The *Mef2c*-deficient model provides a promising alternative rescue scenario as
542 global BMP overactivation was deemed unlikely to overcome the block of cardiomyocyte
543 differentiation resulting from the deficiency of *mef2* protein function. In these experiments,
544 we injected embryos from *Tg(hsp70l:bmp2b)* founders with *mef2c/d*-MO or maintained
545 *Tg(hsp70l:bmp2b)* embryos as a non-injected control group. Injected and non-injected
546 embryos were then heat-shock treated at early (10 hpf), mid (15 hpf), or late somitogenesis
547 (20 hpf) and thyroid and cardiac markers were analyzed in the different treatment groups at
548 28 hpf (**Figure 10**). In the non-injected control embryos, we observed changes in thyroid and
549 cardiac development (**Figure 10A-G**) that were very similar to the effects seen in DMSO-

550 treated control embryos in the previous experimental series (**Figure 9A-G**). Depending on
551 the timing of heat-shock treatment, we observed ectopic expansions of *nkx2.4b* expression
552 along the anterior-posterior axis (heat-shock at 10 hpf) or moderately enhanced *nkx2.4b*
553 expression when heat-shock was applied at mid (15 hpf) or late somitogenesis stages (20
554 hpf). In addition to the irregular shape and position of the thyroidal *nkx2.4b* expression
555 domain, we noted again abnormal *myl7* expression domains, irregularly extending along the
556 anterior-posterior axis (**Figure 10C**).

557 WISH analyses of the thyroid and cardiac marker expression of *Mef2c*-deficient embryos at
558 28 hpf showed a marked reduction in the thyroid *nkx2.4b* staining (**Figure 10H**). The
559 severity of the thyroid specification defects correlated with the severity of a concurrent
560 cardiac developmental phenotype, as judged from the expression of *myl7*. As expected,
561 irrespective of their timing, heat-shocks of non-transgenic *Mef2c*-deficient embryos failed to
562 rescue the thyroid or cardiac phenotype (**Figure 10I,K,M**). In *Mef2c*-deficient embryos
563 carrying the *hsp70l:bmp2b* transgene, heat-shock induction of BMP signaling at early
564 somitogenesis (10 hpf) resulted in a robust thyroid *nkx2.4b* expression, even though the
565 thyroid's shape and position were abnormal (**Figure 10J**). This phenotype largely resembled
566 the expansion along the anterior-posterior axis seen in control embryos heat-shocked at 10 hpf
567 (**Figure 10C**). Similar to the series of heat-shock experiments performed on BIO-treated
568 embryos, a partial rescue of thyroid specification defects was generally limited to heat-shock
569 induction of BMP signaling at early somitogenesis stages. In *Mef2c*-deficient embryos
570 carrying the *hsp70l:bmp2b* transgene, heat-shock induction of BMP signaling at mid- (15
571 hpf) or late somitogenesis (20 hpf) only mildly increased levels of *nkx2.4b* expression
572 compared to untreated *mef2c/d* morphants (**Figure 10L,N**). Compared to the thyroid rescue
573 observed in BIO-treated embryos, a notable difference in the *Mef2c*-deficient model was that
574 heat-shock induction of BMP signaling did not rescue the cardiac differentiation phenotype.

575 Thus, our observations in the cardiac deficient *mef2c/d* morphant model indicate that
576 ectopically induced BMP signaling is sufficient to rescue the thyroid specification defect even
577 in the absence of cardiomyocyte differentiation.

578 **Discussion**

579 In this study, we described severe defects in early zebrafish thyroid development as a
580 result of globally modulated canonical Wnt signaling during gastrula and early somitogenesis
581 stages. While thyroid dysgenesis in response to drug-induced Wnt signaling modulation was
582 first detected in the course of our recent small molecule screening study with zebrafish
583 embryos (21), the current study provides corroborative evidence that the thyroid specification
584 defects observed following treatment with BIO and AZA are due to the up-regulation of
585 canonical Wnt signaling. We used a well-characterized zebrafish biosensor line (35) to
586 confirm that BIO and AZA treatments are effectively inducing canonical Wnt signaling *in*
587 *vivo* during zebrafish development. Our results are, therefore, in line with numerous studies in
588 zebrafish, *Xenopus*, and mammalian cell systems utilizing these two compounds to globally
589 induce Wnt signaling (35), (59), (60). Importantly, the thyroid specification defects observed
590 in drugged embryos were faithfully reproduced in a genetic zebrafish, thereby corroborating
591 critical evidence that the thyroid defects are indeed caused by enhanced Wnt signaling and are
592 not due to possible non-specific side effects of drug treatments.

593 Thyroid phenotyping of drugged embryos at the thyroid anlage stage (28 hpf), using
594 *nkx2.4b* expression as a proxy for thyroid lineage commitment, revealed concentration-
595 dependent losses of *nkx2.4b*-expressing cells in the prospective thyroid region. In zebrafish
596 embryos, thyroidal expression of *nkx2.4b* typically becomes detectable at around 23/24 hpf,
597 and a global assessment of developmental timing in drugged embryos indicated that reduced
598 detection of *nkx2.4b* expression was not solely due to delayed development. Remarkably,
599 gastrula treatment with a high concentration (5 μ M) of BIO or AZA caused a complete
600 absence of detectable *nkx2.4b* expression in 28 hpf embryos. Although the latter phenotype
601 was highly penetrant at 28 hpf (affecting almost 100% of drugged embryos), analyses of
602 treated embryos at later stages (55 hpf) showed that almost all treated embryos developed at

603 least a very tiny thyroid primordium comprised of very few cells expressing the early
604 functional thyroid marker *tg*. It is currently unknown if these few remaining *tg*-expressing
605 thyroid cells at 55 hpf are derived from thyroid precursors expressing *nkx2.4b* at such low
606 levels that are undetectable by our WISH at 28 hpf or if some precursor cells are specified
607 after 28 hpf to give rise to *tg*-expressing thyroid cells. Despite the presence of very few
608 differentiated thyroid cells at later stages, we can conclude that increased canonical Wnt
609 signaling during early zebrafish development impairs the specification of thyroid precursor
610 cells.

611 By progressively shifting the timing of short-term drug treatments, we observed that the
612 primary events leading to this thyroid dysgenesis phenotype occur during gastrula and early
613 somitogenesis stages. Therefore, the question arises whether increased Wnt signaling directly
614 affects development of endodermal progenitors, which later give rise to foregut endoderm and
615 the thyroid cell lineage, or whether indirectly through another cell type (e.g. pre-cardiac
616 mesoderm) that is required later in development as a local source of signals to initiate thyroid
617 specification in the foregut endoderm zebrafish (18), (27).

618 During early vertebrate development, Wnt signaling plays a key role in the anteroposterior
619 patterning, mainly by acting as a posteriorizing factor (61). This anterior-posterior patterning
620 role of Wnt signaling has been extensively studied during neural development (55). In our
621 studies, a robust posteriorizing activity of Wnt on neural development was evident from the
622 severe forebrain and eye development defects. Since the thyroid develops from the anterior
623 foregut endoderm, the posteriorizing activity of Wnt on the endoderm could provide a
624 plausible hypothesis to explain the observed thyroid dysgenesis. Surprisingly few studies
625 have addressed the precise role of Wnt on endoderm patterning. Studies in *Xenopus* embryos
626 indicated that canonical Wnt signaling during gastrulation might pattern the endoderm in a
627 way much similar to what is known for the nervous system (27). Notably, forced Wnt8

628 expression in cells fated to become endoderm was found to block anterior endoderm
629 development in *Xenopus* embryos, resulting in specification failure of foregut organ
630 primordia. In contrast to the aforementioned *Xenopus* studies, morphological and molecular
631 analyses of thyroid-lacking zebrafish embryos revealed the formation of a morphologically
632 fairly normal anterior endoderm with a foregut identity (*foxa2* expression) and confirmed
633 timely expression of various other foregut organ markers (*hhex*, *pdx1*, *prox1a*). Moreover,
634 data presented by McLin *et al.* (27) indicate that thyroid specification was preserved in
635 *Xenopus* embryos if enhanced β -catenin signaling was cell-autonomously restricted to the
636 endoderm lineage. When comparing these study results with our observations, we conclude
637 that posteriorization effects of BIO-induced Wnt activity were by far not as dramatic as
638 reported in the *Xenopus* studies and that posteriorization of anterior endoderm patterning was
639 likely not the primary cause for the severe thyroid specification defects in zebrafish embryos.

640

641 Another striking effect of drug-induced Wnt activation was a severe impairment of
642 cardiac differentiation. Consistent with previous studies, we confirmed that enhanced Wnt
643 signaling during zebrafish gastrulation in zebrafish limits cardiac differentiation within pre-
644 cardiac mesoderm (25), (26). Intriguingly, we observed a close correlation between the
645 disruption of cardiac progenitor differentiation and the thyroid abnormalities. This was true
646 for experiments involving increasing concentrations of BIO and AZA as well as for
647 experiments with different treatment periods. In this respect, it is noteworthy that treatment
648 periods, which caused little if any global posteriorization effects, still showed reduced cardiac
649 differentiation concurrent with thyroid specification defects. Thus, the apparent relationship
650 between the diminished formation of cardiac tissue and the corresponding defects in thyroid
651 specification led us to formulate the hypothesis that the primary effect of enhanced Wnt
652 signaling might be the blockage of cardiac differentiation while the thyroid defects might be a

653 secondary event resulting from a reduction of cardiac-borne signaling cues. This hypothesis is
654 supported by results from several previous studies in different vertebrate models, which
655 provided evidence for a critical role of pre-cardiac and cardiac mesoderm in the induction of
656 thyroid precursor cells signaling (17), (18).

657 Our own studies provided further supporting lines of evidence for this hypothesis by showing
658 that a similar correlation between impaired cardiogenesis and defective thyroid specification
659 exists in *Mef2c*-deficient embryos (52), a model in which heart formation is blocked
660 independent of perturbations in Wnt signaling. Since the mesoderm, and not the foregut
661 endoderm, expresses *mef2ca* and *mef2cb*, this model provided more direct evidence for the
662 contention that thyroid specification relies on proper differentiation of cardiac tissue. A role
663 of mesoderm as a source of signals coming to induce specification of thyroid progenitors
664 within the foregut endoderm is also consistent with what has been already described
665 concerning the specification of other endoderm-derived organs (62), (63), (64).

666

667 While these observations strongly suggest an important role of cardiac mesoderm as a signal
668 source involved in the early steps of thyroid development, it raises the question of the nature
669 of the signaling cues involved in this tissue-tissue interaction. Based on results from our small
670 molecule screening (21) and previous studies in several other model systems, BMP signaling
671 was deemed a primary candidate of particular importance for thyroid specification (65). *In*
672 *vitro* experiments with murine stem cell models identified key conserved roles for BMP
673 signaling in regulating thyroid lineage specification from foregut endoderm (65). On the other
674 hand, Wnt was not required for thyroid specification from endoderm *in vitro*, like it had been
675 previously suggested (66). Expression profiles during embryogenesis also support a potential
676 role of BMP signaling as a key factor in regulating early steps of thyroid development. In
677 mouse, BMP4 is the Bmp ligand expressed at high levels by the cardiac mesoderm, in

678 particular within the secondary heart field, the structure that gives rise among others to the
679 outflow tract, which the developing thyroid lies nearby (67), (68).

680 Danesh *et al.* also demonstrated in mouse embryos that BMPR1a is highly expressed
681 in regions of the pharyngeal endoderm, where endodermal progenitors will differentiate into
682 thyroid cells (68). Thus, Bmp4 could be one critical endogenous Bmp ligand acting from
683 mesoderm to endoderm to initiate thyroid development through interaction with its receptor
684 Bmpr1a. For zebrafish, we further confirmed a high *bmp4* expression in cardiac mesoderm
685 around the time of thyroid specification (Supplementary Figure 5) and ectopic BMP
686 signaling during somitogenesis caused an expansion of the thyroid anlage (Figures 9 & 10).

687

688 Against this background, it is noteworthy that timed overactivation of BMP signaling during
689 zebrafish somitogenesis stages could partially restore thyroid specification in both models of
690 impaired cardiac development. Interestingly, in our model of cardiac dysgenesis due to
691 enhanced Wnt signaling, the restoration of thyroidal *nkx2.4b* expression achieved by
692 subsequent BMP overactivation appeared strictly dependent on a concurrent rescue of cardiac
693 cell differentiation. At this stage, it is therefore not possible to conclude if thyroid
694 specification was directly restored by the ectopic BMP activity in this model. Several lines of
695 evidence indicate that thyroid specification requires the combined action of BMP and FGF
696 signaling (17), (18), (31), (65), (57). One possible interpretation might be that BMP signaling
697 alone might not be sufficient to induce thyroid specification in embryos with almost no
698 cardiac mesoderm formation. In contrast, restoration to some extent of cardiac differentiation
699 by transient BMP overactivation could provide a source of endogenous BMP, FGF, and
700 possibly other signaling cues to induce thyroid specification.

701 Rescue of thyroid specification was also evident in *Mef2c*-deficient embryos after BMP
702 overactivation. However, in this model, the correlation between thyroid rescue and the

703 presence of cardiac mesoderm was less explicit. This correlation reduction was due to the
704 incomplete penetrance of the cardiac phenotype in morphant embryos. However, we observed
705 many *Mef2c*-deficient embryos presenting a partial thyroid rescue while still lacking
706 cardiomyocytes. These observations indicate that ectopic BMP activation might indeed
707 restore thyroid specification even in the absence of detectable cardiomyocytes. To understand
708 the differences between the thyroid rescue induced by ectopic BMP activity in the two cardiac
709 dysgenesis models, the different mechanisms leading to deficient cardiomyocyte development
710 need to be taken into account. Enhanced Wnt signaling at early stages leads to a block of early
711 cardiac mesoderm differentiation with a pronounced deficit in cardiac progenitor
712 differentiation (see Figure 5). In contrast, studies by Hinitz *et al* (52) showed that early
713 cardiac development is uncompromised in *Mef2c*-deficient embryos and that the last steps
714 involved in cardiomyocyte differentiation are blocked in this model, including the up-
715 regulation of *bmp4* expression in the cardiac field. Thus, pre-cardiac mesoderm present in
716 *Mef2c*-deficient embryos might serve as a source of FGF and other signaling factors needed
717 to act in concert with BMP to induce thyroid specification. Given that *Mef2c*-deficient
718 embryos lack *bmp4* expression in the cardiac mesoderm and that ectopic overexpression of
719 *mef2cb* mRNA can induce *bmp4* in the cardiac field (52), it would be interesting to
720 investigate further this model, respect to the expression of other potential thyroid-inducing
721 pathways (e.g., FGF) and their role in acting together with BMP signaling in the process of
722 thyroid specification. Also, results obtained in *Mef2c*-deficient embryos indicate that the
723 thyroid of *Bmp4*-deficient embryo models might bring further insights into the role of BMP
724 signaling in thyroid specification.

725

726 In summary, our studies confirmed and validated our previous results from a small molecule
727 screen that enhanced Wnt signaling during gastrulation stages results in severe inhibition of

728 thyroid specification. Moreover, we provide corroborating evidence for the contention that
729 this thyroid dysgenesis results from a blockage of cardiac development and, consequently, the
730 lack of instructive cardiac-derived signaling cues for the specification of thyroid precursor
731 cells. This hypothesis is supported by a similar perturbation of thyroid specification in *Mef2c*-
732 deficient embryos displaying a lack of cardiomyocyte differentiation. Finally, we demonstrate
733 that ectopic activation of BMP signaling can partially rescue these thyroid phenotypes
734 identifying BMP signaling as one critical component of this tissue-tissue interaction.

735 **Acknowledgments**

736 **Acknowledgments**

737 We thank J.-M. Vanderwinden from the Light Microscopy Facility for technical assistance.

738 This work was supported by grants from the Belgian National Fund for Scientific Research

739 (FNRS) (FRSM 3-4598-12; CDR-J.0145.16), the Action de Recherche Concertée (ARC) de

740 la Communauté Française de Belgique (ARC AUWB-2012-12/17-ULB3), the Fonds

741 d'Encouragement à la Recherche de l'Université Libre de Bruxelles (FER-ULB), the Fund

742 Yvonne Smits (King Baudouin Foundation) and the Berlin Institute of Health (BIH, CRG-

743 TP2).

744 This work was supported by grant the Belgian National Fund for Scientific Research

745 (FNRS): I.V. is FNRS Research Fellow, B.H. and P.G. are Fund for Research in the Industry

746 and the Agriculture (FRIA) research fellow, R.O. was FNRS Postdoctoral fellow and S.C. is

747 FNRS Senior Research Associate. We greatly appreciate the help of J. Bakkers, E. Moro, S.

748 Abdelilah-Seyfried and G. Weidinger for providing us with transgenic lines used in this study.

749 J. Bakkers for *Tg(kdrl:EGFP)* and *Tg(myf17:EGFP)* lines, E. Moro for *Tg(7xTCF-*

750 *Xla.Siam:GFP)*, S. Abdelilah-Seyfried For *Tg(hsp70l:bmp2b)* line, G. Weidinger For

751 *Tg(hsp70l:wnt8a-EGFP)*

752

753 **Disclosure Statement**

754 The authors have nothing to disclose.

755

756 **Corresponding author**

757 Please address all correspondences and requests for reprints to:

758 Sabine Costagliola, Institut de Recherche Interdisciplinaire en Biologie Humaine et
759 Moléculaire, Université Libre de Bruxelles, 808 Route de Lennik, 1070 Brussels, Belgium.

760 Email: scostag@ulb.ac.be.

Robert Opitz, Institute of Experimental Pediatric Endocrinology, Charité Universitätsmedizin
Berlin, Augustenburger Platz 1, 13353, Berlin, Germany.

761 Email: robert.opitz@charite.de.

762

763 **References**

- 764 1. De Felice M, Di Lauro R 2004 Thyroid Development and Its Disorders: Genetics
765 and Molecular Mechanisms. *Endocrine Reviews* **25**:722-746.
- 766 2. Fagman H, Nilsson M 2011 Morphogenetics of early thyroid development. *Journal*
767 *of Molecular Endocrinology* **46**:R33-R42.
- 768 3. Deladoey J, Ruel J, Giguere Y, Van Vliet G 2011 Is the incidence of congenital
769 hypothyroidism really increasing? A 20-year retrospective population-based
770 study in Quebec. *J Clin Endocrinol Metab* **96**:2422-2429.
- 771 4. Vassart G, Dumont JE 2005 Thyroid dysgenesis: multigenic or epigenetic ... or
772 both? *Endocrinology* **146**:5035-5037.
- 773 5. Opitz R, Maquet E, Huisken J, Antonica F, Trubiroha A, Pottier G, Janssens V,
774 Costagliola S 2012 Transgenic zebrafish illuminate the dynamics of thyroid
775 morphogenesis and its relationship to cardiovascular development. *Dev Biol*
776 **372**:203-216.
- 777 6. Lieschke GJ, Currie PD 2007 Animal models of human disease: zebrafish swim
778 into view. *Nature Reviews Genetics* **8**:353-367.
- 779 7. Elsalini OA, Gartzon Jv, Cramer M, Rohr KB 2003 Zebrafish *hhx*, *nk2.1a*, and
780 *pax2.1* regulate thyroid growth and differentiation downstream of Nodal-
781 dependent transcription factors. *Dev Biol* **263**:67-80.
- 782 8. Alt B, Reibe S, Feitosa NM, Elsalini OA, Wendl T, Rohr KB 2006 Analysis of origin
783 and growth of the thyroid gland in zebrafish. *Developmental dynamics*
784 **235**:1872-1883.
- 785 9. Porazzi P, Calebiro D, Benato F, Tiso N, Persani L 2009 Thyroid gland
786 development and function in the zebrafish model. *Molecular and Cellular*
787 *Endocrinology* **312**:14-23.
- 788 10. Manoli M, Driever W 2014 *nkx2.1* and *nkx2.4* genes function partially redundant
789 during development of the zebrafish hypothalamus, preoptic region, and
790 pallidum. *Front Neuroanat* **8**:145.
- 791 11. De Felice M, Di Lauro R 2011 Minireview: Intrinsic and extrinsic factors in
792 thyroid gland development: an update. *Endocrinology* **152**:2948-2956.
- 793 12. Trubiroha A, Gillotay P, Giusti N, Gacquer D, Libert F, Lefort A, Haerlingen B, De
794 Deken X, Opitz R, Costagliola S 2018 A Rapid CRISPR/Cas-based Mutagenesis
795 Assay in Zebrafish for Identification of Genes Involved in Thyroid Morphogenesis
796 and Function. *Sci Rep* **8**:5647.

- 797 **13.** Fagman H, Nilsson M 2010 Morphogenesis of the thyroid gland. *Mol Cell*
798 *Endocrinol* **323**:35-54.
- 799 **14.** Alt B, Elsalini OA, Schrupf P, Haufs N, Lawson N, Schwabe G, Mundlos S, Grüters
800 A, Krude H, Rohr KB 2006 Arteries define the position of the thyroid gland during
801 its developmental localisation. *Development* **133**.
- 802 **15.** Opitz R, Hitz MP, Vandernoot I, Trubiroha A, Abu-Khudir R, Samuels M, Desilets V,
803 Costagliola S, Andelfinger G, Deladoey J 2015 Functional zebrafish studies based
804 on human genotyping point to netrin-1 as a link between aberrant cardiovascular
805 development and thyroid dysgenesis. *Endocrinology* **156**:377-388.
- 806 **16.** Olivieri A, Stazi M, Mastroiacovo P, Fazzini C, Medda E, Spagnolo A, De Angelis S,
807 Grandolfo M, Taruscio D, Cordeddu V, Sorcini M, Hypothyroidism SGfC 2002 A
808 population-based study on the frequency of additional congenital malformations
809 in infants with congenital hypothyroidism: data from the Italian Registry for
810 Congenital Hypothyroidism (1991-1998). *Journal of Clinical Endocrinology and*
811 *Metabolism* **87**:557-562.
- 812 **17.** Wendl T, Adzic D, Schoenebeck J, Scholpp S, Brand M, Yelon D, Rohr K 2007 Early
813 developmental specification of the thyroid gland depends on hox-expressing
814 surrounding tissue and on FGF signals. *Development* **134**:2871-2879.
- 815 **18.** Lania G, Zhang Z, Huynh T, Caprio C, Moon AM, Vitelli F, Baldini A 2009 Early
816 thyroid development requires a Tbx1-Fgf8 pathway. *Dev Biol* **328**:109-117.
- 817 **19.** Porazzi P, Marelli F, Benato F, de Filippis T, Calebiro D, Argenton F, Tiso N,
818 Persani L 2012 Disruptions of global and jagged1-mediated notch signaling affect
819 thyroid morphogenesis in the zebrafish. *Endocrinology* **153**:5645-5658.
- 820 **20.** Stainier DY 2001 Zebrafish genetics and vertebrate heart formation. *Nature*
821 *reviews* **2**:39-48.
- 822 **21.** Haerlingen B, Opitz R, Vandernoot I, Trubiroha A, Gillotay P, Giusti N, Costagliola
823 S 2019 Small-Molecule Screening in Zebrafish Embryos Identifies Signaling
824 Pathways Regulating Early Thyroid Development. *Thyroid*.
- 825 **22.** Steinhart Z, Angers S 2018 Wnt signaling in development and tissue homeostasis.
826 *Development* **145**.
- 827 **23.** He X, Semenov M, Tamai K, Zeng X 2004 LDL receptor-related proteins 5 and 6 in
828 Wnt/beta-catenin signaling: arrows point the way. *Development* **131**:1663-1677.
- 829 **24.** Gordon MD, Nusse R 2006 Wnt signaling: multiple pathways, multiple receptors,
830 and multiple transcription factors. *J Biol Chem* **281**:22429-22433.
- 831 **25.** Dohn TE, Waxman JS 2012 Distinct phases of Wnt/beta-catenin signaling direct
832 cardiomyocyte formation in zebrafish. *Dev Biol* **361**:364-376.
- 833 **26.** Ueno S, Weidinger G, Osugi T, Kohn AD, Golob JL, Pabon L, Reinecke H, Moon RT,
834 Murry CE 2007 Biphasic role for Wnt/beta-catenin signaling in cardiac
835 specification in zebrafish and embryonic stem cells. *Proc Natl Acad Sci U S A*
836 **104**:9685-9690.
- 837 **27.** McLin VA, Rankin SA, Zorn AM 2007 Repression of Wnt/beta-catenin signaling in
838 the anterior endoderm is essential for liver and pancreas development.
839 *Development* **134**:2207-2217.
- 840 **28.** Poulain M, Ober EA 2011 Interplay between Wnt2 and Wnt2bb controls multiple
841 steps of early foregut-derived organ development. *Development* **138**:3557-3568.
- 842 **29.** Westerfield M 2000 *The zebrafish book. A guide for the laboratory use of*
843 *zebrafish (Danio rerio)*. University of Oregon press **4th ed. Eugene, OR**.
- 844 **30.** Kimmel CBea 1995 Stages of embryonic development of the zebrafish.
845 *Developmental dynamics* **203**:253-310.

- 846 **31.** Longmire TA, Ikonomou L, Hawkins F, Christodoulou C, Cao Y, Jean JC, Kwok LW,
847 Mou H, Rajagopal J, Shen SS, Downton AA, Serra M, Weiss DJ, Green MD, Snoeck
848 HW, Ramirez MI, Kotton DN 2012 Efficient derivation of purified lung and thyroid
849 progenitors from embryonic stem cells. *Cell Stem Cell* **10**:398-411.
- 850 **32.** White R, Sessa A, Burke C, Bowman T, LeBlanc J, Ceol C, Bourque C, Dovey M,
851 Goessling W, Burns C, Zon L 2008 Transparent adult zebrafish as a tool for in vivo
852 transplantation analysis. *Cell Stem Cell* **2**:183-189.
- 853 **33.** Jin SW, Herzog W, Santoro MM, Mitchell TS, Frantsve J, Jungblut B, Beis D, Scott
854 IC, D'Amico LA, Ober EA, Verkade H, Field HA, Chi NC, Wehman AM, Baier H,
855 Stainier DY 2007 A transgene-assisted genetic screen identifies essential
856 regulators of vascular development in vertebrate embryos. *Dev Biol* **307**:29-42.
- 857 **34.** Huang CJ, Tu CT, Hsiao CD, Hsieh FJ, Tsai HJ 2003 Germ-line transmission of a
858 myocardium-specific GFP transgene reveals critical regulatory elements in the
859 cardiac myosin light chain 2 promoter of zebrafish. *Dev Dyn* **228**:30-40.
- 860 **35.** Moro E, Ozhan-Kizil G, Mongera A, Beis D, Wierzbicki C, Young RM, Bournele D,
861 Domenichini A, Valdivia LE, Lum L, Chen C, Amatruda JF, Tiso N, Weidinger G,
862 Argenton F 2012 In vivo Wnt signaling tracing through a transgenic biosensor
863 fish reveals novel activity domains. *Developmental Biology* **366**:327-340.
- 864 **36.** Mizoguchi T, Verkade H, Heath JK, Kuroiwa A, Kikuchi Y 2008 Sdf1/Cxcr4
865 signaling controls the dorsal migration of endodermal cells during zebrafish
866 gastrulation. *Development* **135**:2521-2529.
- 867 **37.** Chocron S, Verhoeven MC, Rentzsch F, Hammerschmidt M, Bakkers J 2007
868 Zebrafish Bmp4 regulates left-right asymmetry at two distinct developmental
869 time points. *Dev Biol* **305**:577-588.
- 870 **38.** Weidinger G, Thorpe C, Wuennenberg-Stapleton K, Ngai J, Moon R 2005 The Sp1-
871 related transcription factors sp5 and sp5-like act downstream of Wnt/beta-
872 catenin signaling in mesoderm and neurectoderm patterning. *Current Biology*
873 **29**:489-500.
- 874 **39.** Karlsson J, Hofsten Jv, Olsson P-E 2001 Generating Transparent Zebrafish: A
875 Refined Method to Improve Detection of Gene Expression During Embryonic
876 Development. *Marine Biotechnology* **3**:522-527.
- 877 **40.** Meijer L, Flajolet M, Greengard P 2004 Pharmacological inhibitors of glycogen
878 synthase kinase 3. *Trends Pharmacol Sci* **25**:471-480.
- 879 **41.** Chen B, Dodge ME, Tang W, Lu J, Ma Z, Fan CW, Wei S, Hao W, Kilgore J, Williams
880 NS, Roth MG, Amatruda JF, Chen C, Lum L 2009 Small molecule-mediated
881 disruption of Wnt-dependent signaling in tissue regeneration and cancer. *Nat*
882 *Chem Biol* **5**:100-107.
- 883 **42.** Shin D, Shin CH, Tucker J, Ober EA, Rentzsch F, Poss KD, Hammerschmidt M,
884 Mullins MC, Stainier DY 2007 Bmp and Fgf signaling are essential for liver
885 specification in zebrafish. *Development* **134**:2041-2050.
- 886 **43.** Yelon D, Horne S, Stainier D 1999 Restricted expression of cardiac myosin genes
887 reveals regulated aspects of heart tube assembly in zebrafish. *Dev Biol* **214**:23-
888 37.
- 889 **44.** Yelon D, Ticho B, Halpern M, Ruvinsky I, Ro R, Silver L, Stainier D 2000 The bHLH
890 transcription factor hand2 plays parallel roles in zebrafish heart and pectoral fin
891 development. *Development* **127**:2573-2582.
- 892 **45.** Liao E, Paw B, Oates A, Pratt S, Postlethwait J, Zon L 1998 SCL/Tal-1 transcription
893 factor acts downstream of cloche to specify hematopoietic and vascular
894 progenitors in zebrafish. *Genes Development* **12**:621-626.

- 895 46. Thisse CT, B. 2008 High-resolution in situ hybridization to whole-mount
896 zebrafish embryos. *Nat Protoc* **3**:59-69.
- 897 47. Opitz R, Maquet E, Zoenen M, Dadhich R, Costagliola S 2011 TSH Receptor
898 Function Is Required for Normal Thyroid Differentiation in Zebrafish. *Molecular*
899 *Endocrinology* **25**:1579-1599.
- 900 48. Dorsky RI, Sheldahl LC, Moon RT 2002 A transgenic Lef1/beta-catenin-
901 dependent reporter is expressed in spatially restricted domains throughout
902 zebrafish development. *Dev Biol* **241**:229-237.
- 903 49. Pfaffl M 2001 A new mathematical model for relative quantification in real-time
904 RT-PCR. *Nucleic Acids Research* **29**:e45.
- 905 50. Tang R, Dodd A, Lai D, McNabb W, Love D 2007 Validation of zebrafish (*Danio*
906 *rerio*) reference genes for quantitative real-time RT-PCR normalization. *Acta*
907 *Biochim Biophys Sin (Shangai)* **39**:384-390.
- 908 51. Hinitz Y, Hughes SM 2007 Mef2s are required for thick filament formation in
909 nascent muscle fibres. *Development* **134**:2511-2519.
- 910 52. Hinitz Y, Pan L, Walker C, Dowd J, Moens CB, Hughes SM 2012 Zebrafish Mef2ca
911 and Mef2cb are essential for both first and second heart field cardiomyocyte
912 differentiation. *Dev Biol* **369**:199-210.
- 913 53. van de Water S, van de Wetering M, Joore J, Esseling J, Bink R, Clevers H, Zivkovic
914 D 2001 Ectopic Wnt signal determines the eyeless phenotype of zebrafish
915 masterblind mutant. *Development* **128**:3877-3888.
- 916 54. Yamaguchi TP 2001 Heads or tails: Wnts and anterior-posterior patterning. *Curr*
917 *Biol* **11**:R713-724.
- 918 55. Green D, Whitener A, Mohanty S, Lekven A 2015 Vertebrate nervous system
919 posteriorization: Grading the function of Wnt signaling. *Dev Dyn* **244**:507-512.
- 920 56. Manfroid I, Delporte F, Baudhuin A, Motte P, Neumann CJ, Voz ML, Martial JA,
921 Peers B 2007 Reciprocal endoderm-mesoderm interactions mediated by fgf24
922 and fgf10 govern pancreas development. *Development* **134**:4011-4021.
- 923 57. Serra M, Alysandratos KD, Hawkins F, McCauley KB, Jacob A, Choi J, Caballero IS,
924 Vedaie M, Kurmann AA, Ikonomou L, Hollenberg AN, Shannon JM, Kotton DN
925 2017 Pluripotent stem cell differentiation reveals distinct developmental
926 pathways regulating lung- versus thyroid-lineage specification. *Development*
927 **144**:3879-3893.
- 928 58. Kurmann Anita A, Serra M, Hawkins F, Rankin Scott A, Mori M, Astapova I, Ullas S,
929 Lin S, Bilodeau M, Rossant J, Jean Jyh C, Ikonomou L, Deterding Robin R, Shannon
930 John M, Zorn Aaron M, Hollenberg Anthony N, Kotton Darrell N 2015
931 Regeneration of Thyroid Function by Transplantation of Differentiated
932 Pluripotent Stem Cells. *Cell Stem Cell* **17**:527-542.
- 933 59. Chen EY, DeRan MT, Ignatius MS, Grandinetti KB, Clagg R, McCarthy KM, Lobbardi
934 RM, Brockmann J, Keller C, Wu X, Langenau DM 2014 Glycogen synthase kinase 3
935 inhibitors induce the canonical WNT/ -catenin pathway to suppress growth and
936 self-renewal in embryonal rhabdomyosarcoma. *Proceedings of the National*
937 *Academy of Sciences* **111**:5349-5354.
- 938 60. Meijer L, Skaltsounis A-L, Magiatis P, Polychronopoulos P, Knockaert M, Leost M,
939 Ryan XP, Vonica CA, Brivanlou A, Dajani R, Crovace C, Tarricone C, Musacchio A,
940 Roe SM, Pearl L, Greengard P 2003 GSK-3-Selective Inhibitors Derived from
941 Tyrian Purple Indirubins. *Chemistry & Biology* **10**:1255-1266.

- 942 **61.** Tuazon FB, Mullins MC 2015 Temporally coordinated signals progressively
943 pattern the anteroposterior and dorsoventral body axes. *Semin Cell Dev Biol*
944 **42**:118-133.
- 945 **62.** Deutsch G, Jung J, Zheng M, Lora J, Zaret KS 2001 A bipotential precursor
946 population for pancreas and liver within the embryonic endoderm. *Development*
947 **128**:871-881.
- 948 **63.** Ober EA, Verkade H, Field HA, Stainier DY 2006 Mesodermal Wnt2b signalling
949 positively regulates liver specification. *Nature* **442**:688-691.
- 950 **64.** Neves H, Dupin E, Parreira L, Le Douarin NM 2012 Modulation of Bmp4 signalling
951 in the epithelial-mesenchymal interactions that take place in early thymus and
952 parathyroid development in avian embryos. *Dev Biol* **361**:208-219.
- 953 **65.** Kurmann AA, Serra M, Hawkins F, Rankin SA, Mori M, Astapova I, Ullas S, Lin S,
954 Bilodeau M, Rossant J, Jean JC, Ikonomidou L, Deterding RR, Shannon JM, Zorn AM,
955 Hollenberg AN, Kotton DN 2015 Regeneration of Thyroid Function by
956 Transplantation of Differentiated Pluripotent Stem Cells. *Cell Stem Cell* **17**:527-
957 542.
- 958 **66.** Goss AM, Tian Y, Tsukiyama T, Cohen ED, Zhou D, Lu MM, Yamaguchi TP,
959 Morrisey EE 2009 Wnt2/2b and beta-catenin signaling are necessary and
960 sufficient to specify lung progenitors in the foregut. *Dev Cell* **17**:290-298.
- 961 **67.** Klaus A, Saga Y, Taketo MM, Tzahor E, Birchmeier W 2007 Distinct roles of
962 Wnt/beta-catenin and Bmp signaling during early cardiogenesis. *Proceedings of*
963 *the National Academy of Sciences of the United States of America* **104**:18531-
964 18536.
- 965 **68.** Danesh SM, Villasenor A, Chong D, Soukup C, Cleaver O 2009 BMP and BMP
966 receptor expression during murine organogenesis. *Gene Expr Patterns* **9**:255-
967 265.
- 968

969

970 **Figure Legends**

971 **Fig. 1. Drug-induced overactivation of canonical Wnt signaling during gastrulation**

972 **impairs thyroid specification. (A-H)** Expression of the early thyroid marker *nkx2.4b* in 28

973 hpf embryos following treatment with 0.1% DMSO (vehicle control) and two Wnt-inducing

974 drugs, BIO and azakenpaullone (AZA) between 6 and 10 hpf. In control embryos (A,B,E,F),

975 *nkx2.4b* is expressed in the thyroid anlage (T) and the ventral forebrain (hypothalamus, H). In

976 response to BIO (C-D) and AZA (G-H) treatment, *nkx2.4b* mRNA expression is lost in both

977 domains in the majority of embryos. Arrows point to *nkx2.4b* expression in the thyroid

978 anlage. Dorsal views with anterior oriented to the top (A,C,E,G) and lateral views with

979 anterior oriented to the left (B,D,F,H) are shown. (I): Quantification of the proportion of

980 specimen displaying thyroid specification defects following AZA treatment, as determined by
981 *nkx2.4b* staining of 28 hpf embryos. Results are presented as the percentage of embryos
982 displaying a particular phenotype, showing a concentration-dependent *nkx2.4b* mRNA loss of
983 expression. The total number of specimens analyzed for each treatment group is provided on
984 the top of each column. Scale bar, 200 μ m.

985

986 **Fig. 2. Drug-induced overactivation of canonical Wnt signaling during gastrulation**
987 **impairs the thyroid primordium formation.** (A-H) Expression of the thyroid marker
988 *nkx2.4b* in 55 hpf embryos following treatment with 0.1% DMSO (vehicle control) and the
989 Wnt-inducing drug BIO between 6 and 10 hpf. In control embryos (A,E), *nkx2.4b* is
990 expressed in the thyroid primordium (T) and the ventral forebrain (hypothalamus, H). In
991 response to BIO (B-D,F-H) treatment, *nkx2.4b* mRNA expression is reduced or lost in both
992 tissues in a concentration-dependent manner. Arrows point to *nkx2.4b* expression in the
993 thyroid primordium. Lateral views with anterior oriented to the left (A-D) and dorsal views
994 with anterior oriented to the top (E-H) are shown. (I): Quantification of the percentage of
995 embryos displaying a particular phenotype following BIO treatment, as determined by
996 *nkx2.4b* staining of 55 hpf embryos. Total numbers of specimens analyzed for each treatment
997 group are provided on the top of each column. (J-Q) Expression of the terminal thyroid
998 differentiation marker *tg* in 55 hpf embryos following treatment with 0.1% DMSO (vehicle
999 control) and the Wnt-inducing drug BIO between 6 and 10 hpf. In control embryos (J,N), *tg*
1000 is exclusively expressed in the thyroid primordium (T). In response to BIO treatment (K-
1001 M,O-Q), *tg* mRNA expression is reduced or lost in a concentration-dependent manner.
1002 Arrows point to the thyroid primordium. Lateral views with anterior oriented to the left (J-M)
1003 and dorsal views with anterior oriented to the top (N-Q) are shown. (I): Quantification of the
1004 percentage of embryos displaying a particular phenotype following BIO treatment, as

1005 determined by *tg* staining of 55 hpf embryos. Total numbers of specimens analyzed for each
1006 treatment group are provided on the top of each column. Scale bar, 200 μ m.

1007

1008 **Fig. 3. Heat shock-induced overexpression of *wnt8a-GFP* during gastrulation impairs**
1009 **thyroid specification and thyroid primordium formation.**

1010 **(A,B)** Expression of the thyroid marker *nkx2.4b* in 28 hpf embryos following heat shock
1011 (HS) treatment of *Tg(hsp70l:wnt8a-GFP)* embryos at 6 hpf. In response to HS, embryos
1012 carrying the HS-inducible *wnt8a-GFP* transgene showed a great reduction or even loss of
1013 *nkx2.4b* mRNA expression in the thyroid anlage (T) and the ventral forebrain
1014 (hypothalamus, H), whereas expression of *nkx2.4b* in both tissues was unaffected after HS of
1015 non-transgenic siblings. Dorsal views with anterior oriented to the top are shown. Arrows
1016 point to *nkx2.4b* expression in the thyroid anlage. **(C,D)** Expression of the terminal thyroid
1017 differentiation marker *tg* in 55 hpf embryos following heat shock (HS) treatment of
1018 *Tg(hsp70l:wnt8a-GFP)* embryos at 6 hpf. Note the strongly reduced size of the thyroid
1019 primordium in embryos carrying the HS-inducible *wnt8a-GFP* transgene compared to normal
1020 thyroid size in non-transgenic siblings. Similar to drug-induced wnt overactivation, HS-
1021 induced overexpression of the *wnt8a-GFP* transgene resulted in a dramatic neural
1022 posteriorization phenotype (loss of anterior neural tissue, lack of eyes). Ventral views with
1023 anterior oriented to the top are shown. Arrows point to *tg* expression in the thyroid
1024 primordium. Scale bar, 200 μ m.

1025

1026 **Fig. 4. Overactivation of canonical Wnt signaling during gastrula stages has limited**
1027 **effects on markers of endodermal patterning and endodermal organogenesis. (A-L)**

1028 Comparative whole-mount *in situ* hybridization analysis of mRNA expression patterns for a
1029 panel of markers of endodermal patterning in embryos treated with 0.1% DMSO (vehicle

1030 control) and 5 μ M BIO from 6 – 10 hpf. In contrast to the lack of *nkx2.4b* (**A,B**) and *hhex*
1031 (**C,D**) expression in the region of the thyroid anlage (T) of BIO-treated embryos, *hhex*
1032 expression is maintained in the region of the prospective liver (L) and pancreas (P)
1033 development. Robust *foxa2* expression (**E,F**) in BIO-treated embryos indicates that
1034 specification of foregut endoderm (FE) was not blocked by Wnt overactivation. However,
1035 expression of the mid-/hindgut marker *foxa3* (**G,H**) was expanded towards more anterior
1036 regions in several BIO-treated embryos suggesting possible posteriorization effects on
1037 endodermal patterning. Importantly, BIO-treated embryos displayed robust staining for all
1038 markers of hepatic and pancreatic development including *hhex* (**C,D**), *foxa3* (**G,H**), *pdx1*
1039 (**I,J**) and *prox1a* (**K,L**) while showing a specific reduction or lack of markers of early thyroid
1040 development. Long arrows point to the thyroid, short arrows to the liver, and arrowheads to
1041 pancreatic domains. Brackets in panels **E,F** demarcate the foregut endoderm (FE) domain of
1042 *foxa2* expression. Panels A-J show dorsal views with anterior oriented to the top. Panels K
1043 and L show lateral views with anterior oriented to the left. Scale bar, 200 μ m.
1044

1045 **Fig. 5. Drug-induced overactivation of canonical Wnt signaling during gastrulation**
1046 **impairs early stages of cardiac development.** (A-L) Whole-mount *in situ* hybridization
1047 analysis of mRNA expression for a panel of cardiac differentiation markers in 13 hpf embryos
1048 treated with 0.1% DMSO (vehicle control) and 5 μ M BIO from 6 – 10 hpf. BIO treatment
1049 severely blocked early stages of cardiac development, as shown by the dramatic reduction in
1050 early cardiac markers *nkx2.5* (A,B) and *mef2cb* (C,D). In addition, there is a severe
1051 impairment of endothelial precursor formation, as indicated by the loss of *scl* expression
1052 (E,F) in BIO-treated embryos. Wnt overactivation specifically affected cardiac and
1053 endothelial precursor development, as shown by robust expression of other markers of lateral
1054 plate mesoderm development including *hand2* (G,H), *gata4* (I,J), and *gata5* (K,L). Dorsal
1055 views with anterior oriented to the top are shown. (M-P) Expression analysis of the
1056 myocardial marker *myl7* at 19 hpf reveals concentration-dependent effects of early BIO
1057 treatment on heart morphogenesis, as evident from the impaired cardiac cone formation,
1058 delayed midline fusion of bilateral cardiac fields, and severe depletion of differentiated
1059 cardiomyocytes. Arrows point to *myl7* expression in the region of the forming cardiac cone.
1060 Dorsal views with anterior oriented to the top are shown. Scale bar, 200 μ m.

1061

1062 **Fig. 6. Thyroid specification defects coincide with impaired cardiac development in**
1063 **embryos following drug-induced overactivation of canonical Wnt signaling.** (A-F) Dual-
1064 color whole-mount *in situ* hybridization analysis of mRNA expression of markers for early
1065 thyroid (*nkx2.4b*) and cardiac (*myl7*) development in 28 hpf embryos treated with 0.1%
1066 DMSO (vehicle control) and varying concentrations of BIO from 6-10 hpf. Wnt
1067 overactivation during this period concurrently affected thyroid and cardiac development
1068 though thyroid specification appeared slightly more sensitive to BIO treatment. The severity
1069 of the thyroid defects was tightly correlated to the degree of neural posteriorization effects.

1070 (G-L) Dual-color *in situ* hybridization analysis of *nkx2.4b* and *myl7* expression in 28 hpf
1071 embryos treated with 0.1% DMSO (vehicle control) and varying concentrations of
1072 azakenpaullone (AZA) from 9-12 hpf. Wnt overactivation during this slightly later period
1073 resulted in few if any neural posteriorization phenotypes, whereas thyroid and cardiac
1074 development were concurrently affected, showing a similar sensitivity to perturbed Wnt
1075 signaling. Dorsal views (A,C,E,G,I,K) with anterior to the top and lateral views
1076 (B,D,F,H,J,L) with anterior to the left are shown. Blue arrows point to thyroidal *nkx2.4b*
1077 expression and red arrows to *myl7* expression in the heart tube. Scale bar, 200 μ m
1078

1079 **Fig. 7. Time-dependent effects of Wnt overactivation on thyroid and cardiac**
1080 **development during gastrulation and early somitogenesis stages.**

1081 (A-L) Dual-color whole-mount *in situ* hybridization analysis of mRNA expression of
1082 markers for early thyroid (*nkx2.4b*) and cardiac (*myl7*) development in 28 hpf embryos
1083 treated with 0.1% DMSO (vehicle control) and azakenpaullone (AZA) during different
1084 periods of early development. Note that neural posteriorization phenotypes became much less
1085 prominent and severe when drug-induced Wnt overactivation was initiated at late gastrula
1086 stages. Concurrent defects in thyroid and cardiac development were detected for all drug
1087 treatments that started before 11 hpf. Prevalence and severity of thyroid and cardiac
1088 phenotypes showed a close correlation across different treatment periods. Blue arrows point
1089 to thyroidal *nkx2.4b* expression and red arrows to *myl7* expression in the heart tube. Dorsal
1090 views (A,C,E,G,I,K) with anterior to the top and lateral views (B,D,F,H,J,L) with anterior
1091 to the left are shown. Scale bar, 200 μ m. (M,N) Quantification of the proportion of specimen
1092 displaying defects in thyroid specification (M) and cardiac development (N) following AZA
1093 treatment, as determined by *nkx2.4b* (M) and *myl7* (N) staining of 28 hpf embryos. Results
1094 are presented as the percentage of embryos displaying a particular phenotype. The total

1095 number of specimens analyzed for each treatment group is provided on the top of each
1096 column.

1097

1098 **Fig. 8. Impaired cardiac development in *mef2c/d* morpholino-injected embryos is**
1099 **associated with reduced thyroid marker expression.**

1100 **(A-D)** Dual-color whole-mount *in situ* hybridization analysis of mRNA expression of
1101 markers for early thyroid (*nkx2.4b*) and cardiac (*myl7*) development in 28 hpf embryos
1102 injected with *mef2c/d* morpholino (MO) and non-injected control embryos (NI). MO
1103 injection caused variable loss of differentiated cardiomyocytes and resulted in smaller hearts
1104 **(C)** compared to controls. Concurrently, these embryos displayed reduced staining of *nkx2.4b*
1105 **(C)**. **(E-H)** Dual-color whole-mount *in situ* hybridization analysis of mRNA expression of
1106 *myl7* and the thyroid differentiation marker *tg* in 55 hpf embryos injected with *mef2c/d*
1107 morpholino (MO) and non-injected control embryos (NI). MO-injected embryos displayed
1108 small, string-like midline hearts **(G)** and a modest reduction in *tg* staining **(G)**. Blue arrows
1109 point to thyroidal *nkx2.4b* and *tg* expression and red arrows to *myl7* expression in the heart
1110 tube. Dorsal views **(A,C)** with anterior to the top, lateral views **(B,D,F,H)** with anterior to
1111 the left and ventral views **(E,G)** with anterior to the top are shown. Scale bar, 200 μ m.

1112

1113 **Fig. 9. Conditional overactivation of BMP signaling in *Tg(hsp70l:bmp2b)* embryos**
1114 **partially rescues BIO-induced thyroid specification defects.** **(A-R)** Dual-color whole-
1115 mount *in situ* hybridization analysis of thyroid (*nkx2.4b*) and cardiac (*myl7*) markers in 28
1116 hpf embryos carrying the HS-inducible *bmp2b* transgene (*bmp2b+*) and in non-transgenic
1117 siblings (*bmp2b-*). Panels **A-I** show results for embryos that were treated with 0.1% DMSO
1118 (vehicle control) from 8-11 hpf and were subsequently exposed to timed heat shock (HS)
1119 treatment at early (11 hpf), mid (15 hpf) or late somitogenesis (20 hpf) and for embryos

1120 exposed to repeated HS at 11, 15 and 20 hpf. Carriers of the *bmp2b* transgene showed
1121 enhanced *nkx2.4b* expression in response to HS irrespective of the specific timing of HS
1122 treatment. Note that HS at 11 hpf (**B,C**) and repeated HS treatment (**H,I**) disrupted heart
1123 formation and caused ectopic stretches of *myl7* expression bilateral to the midline. Panels **J-R**
1124 show corresponding effects of HS treatment for embryos that were treated with 5 μ M BIO
1125 from 8-11 hpf. HS of non-transgenic embryos did not affect the BIO-induced deficits in
1126 thyroid and cardiac development (compare **J** to **K,M,O,Q**). Carriers of the *bmp2b* transgene
1127 showed variable levels of *nkx2.4b* expression rescue, depending on the specific timing of HS
1128 treatment. Note that HS at 11 hpf (**K,L**) and the repeated HS treatment (**Q,R**) were most
1129 effective in restoring robust *nkx2.4b* expression. Partial recovery of *myl7* expression was
1130 detectable in response to *bmp2b* overexpression, but heart tube formation was never
1131 restored. Dorsal views with anterior oriented to the top are shown. Blue arrows point to
1132 *nkx2.4b* expression in the thyroid anlage and red arrows to domains of *myl7* expression. Scale
1133 bar: 200 μ m. (**S,T**) Quantification of the proportion of specimens displaying thyroid (**S**) and
1134 cardiac phenotypes (**T**) in response to different HS treatments as determined by *nkx2.4b* (**S**)
1135 and *myl7* (**T**) staining of 28 hpf embryos. Results are presented as the percentage of embryos
1136 displaying a particular phenotype. The total number of specimens analyzed for each treatment
1137 group is provided on the top of each column.

1138

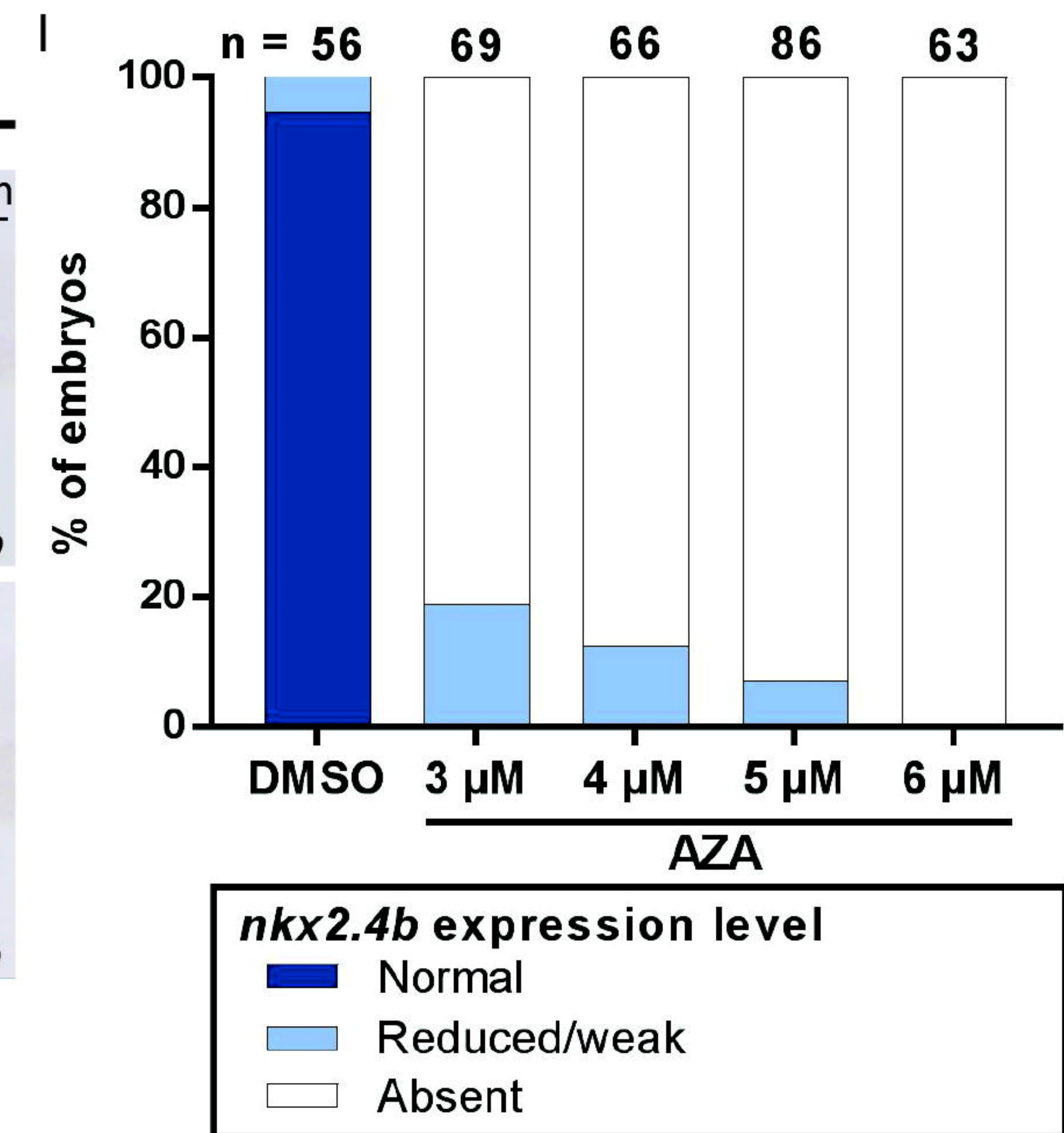
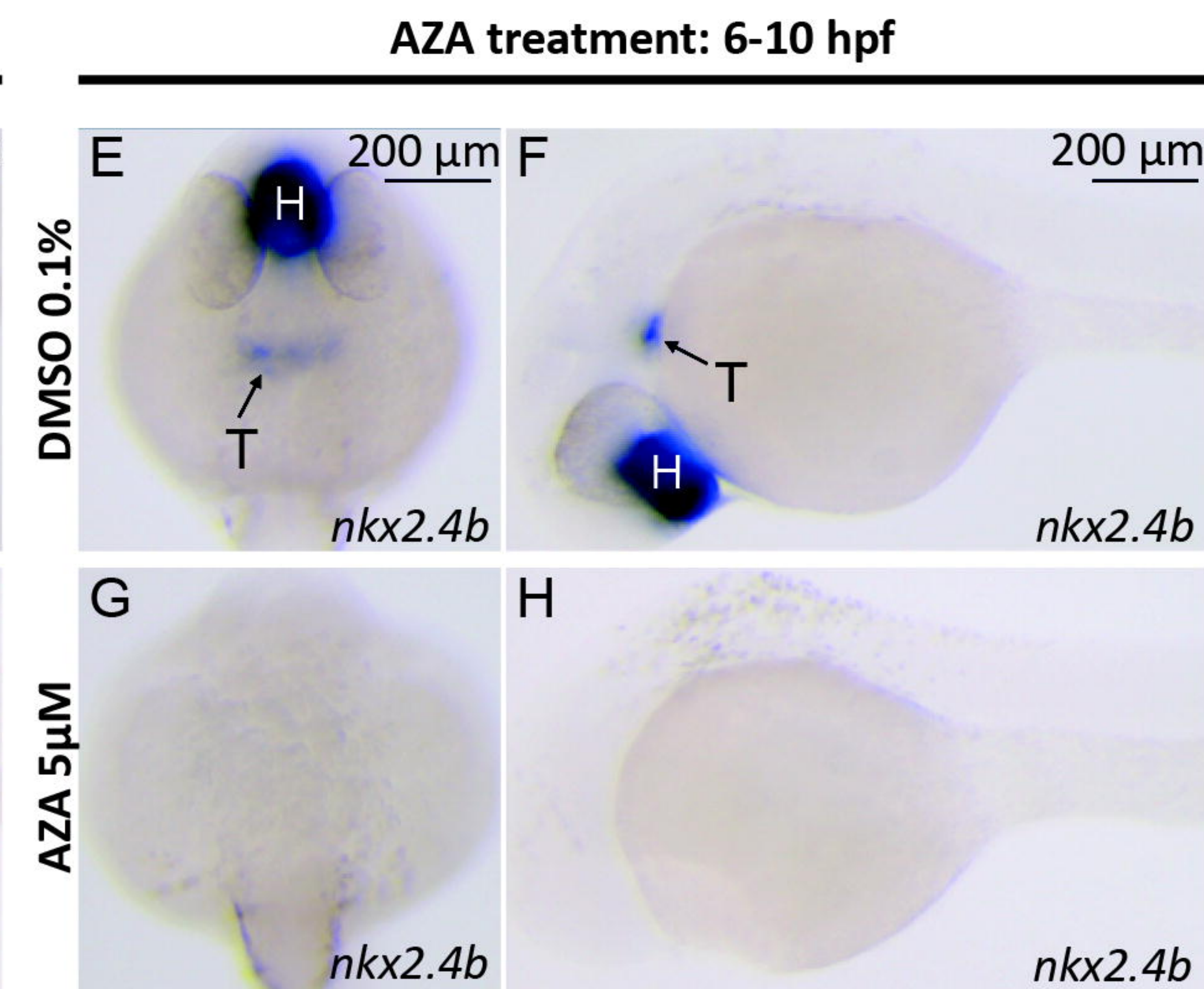
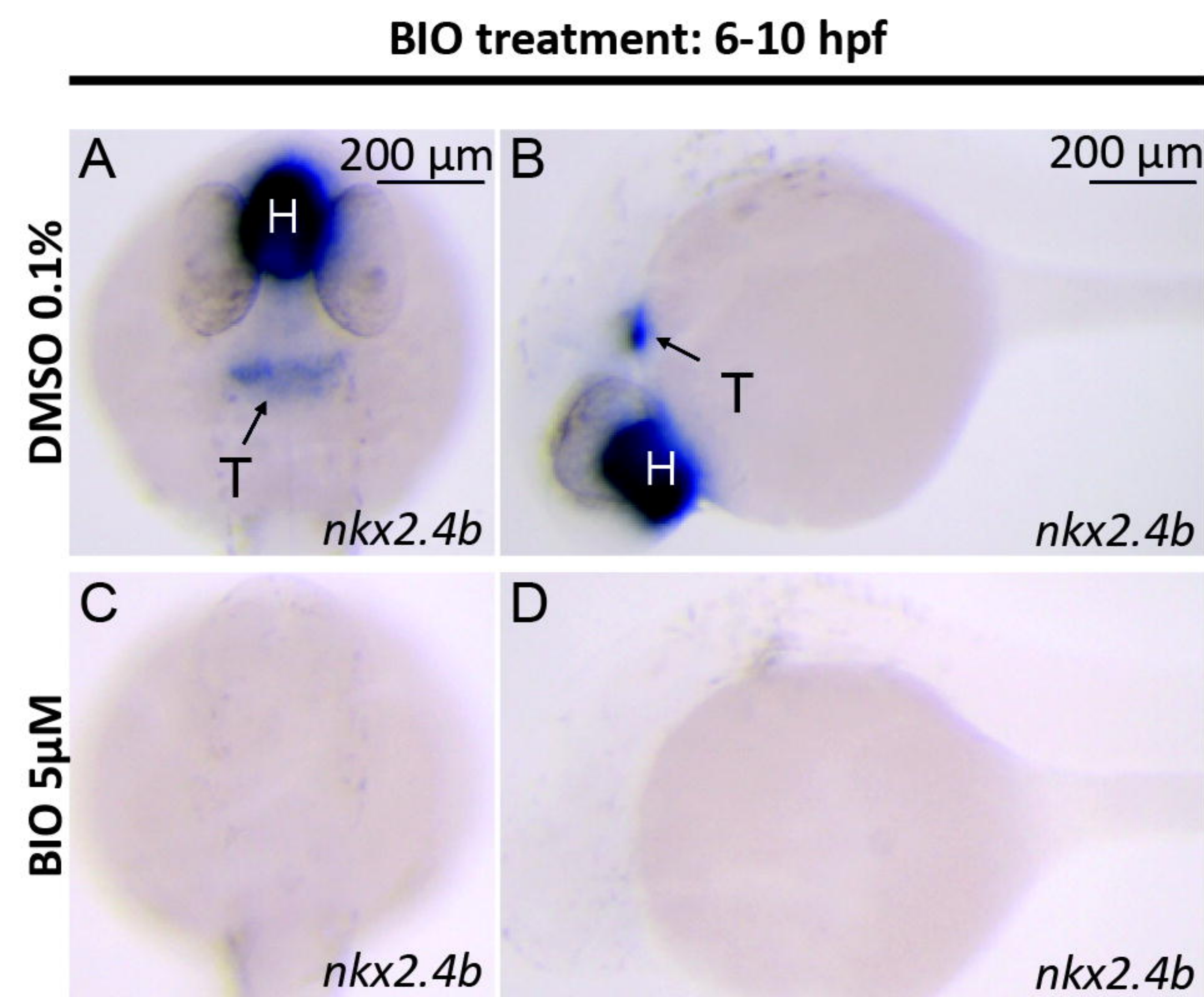
1139 **Fig. 10. Conditional overactivation of BMP signaling in *Tg(hsp70l:bmp2b)* embryos**
1140 **partially rescues *mef2c/d* morpholino-induced thyroid specification defects.**

1141 (**A-N**) Dual-color whole-mount *in situ* hybridization analysis of thyroid (*nkx2.4b*) and
1142 cardiac (*myl7*) markers in 28 hpf embryos carrying the HS-inducible *bmp2b* transgene
1143 (*bmp2b*⁺) and in non-transgenic siblings (*bmp2b*⁻). Panels **A-G** show results for control
1144 embryos exposed to timed heat shock (HS) treatment at early (10 hpf), mid (15 hpf) or late

1145 somitogenesis (20 hpf). Carriers of the *bmp2b* transgene showed enhanced *nkx2.4b*
1146 expression in response to HS irrespective of the specific timing of HS treatment. Note that HS
1147 at 10 hpf (**B,C**) disrupted heart formation and caused ectopic stretches of *myl7* expression
1148 bilateral to the midline. Panels **H-N** show corresponding effects of HS treatment for embryos
1149 that were injected with *mef2c/d* morpholino (MO) at the one-cell stage. HS of non-transgenic
1150 embryos did not affect the MO-induced deficits in thyroid and cardiac development (compare
1151 **H** to **I,K,M**). Carriers of the *bmp2b* transgene showed variable levels of *nkx2.4b* expression
1152 rescue, depending on the specific timing of HS treatment. Note that HS at 10 hpf (**I,J**) was
1153 most effective in restoring robust *nkx2.4b* expression. No significant recovery of *myl7*
1154 expression was detectable in response to *bmp2b* overexpression. Dorsal views with anterior
1155 oriented to the top are shown. Blue arrows point to *nkx2.4b* expression in the thyroid anlage
1156 and red arrows to domains of *myl7* expression. Scale bar: 200 μ m. (**O,P**) Quantification of
1157 the proportion of specimens displaying thyroid (**O**) and cardiac phenotypes (**P**) in response
1158 to different HS treatments as determined by *nkx2.4b* (**O**) and *myl7* (**P**) staining of 28 hpf
1159 embryos. Results are presented as the percentage of embryos displaying a particular
1160 phenotype. The total number of specimens analyzed for each treatment group is provided on
1161 the top of each column.

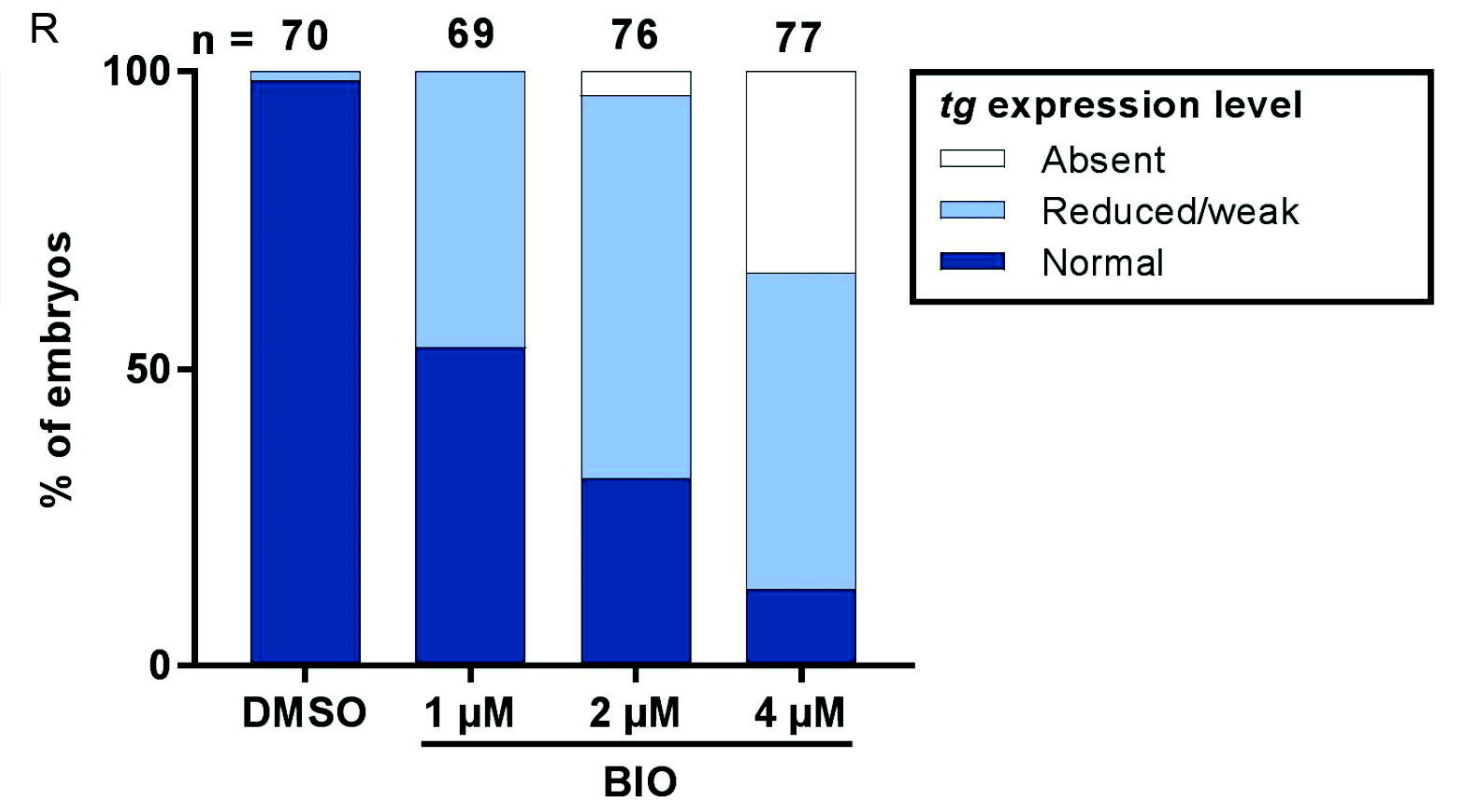
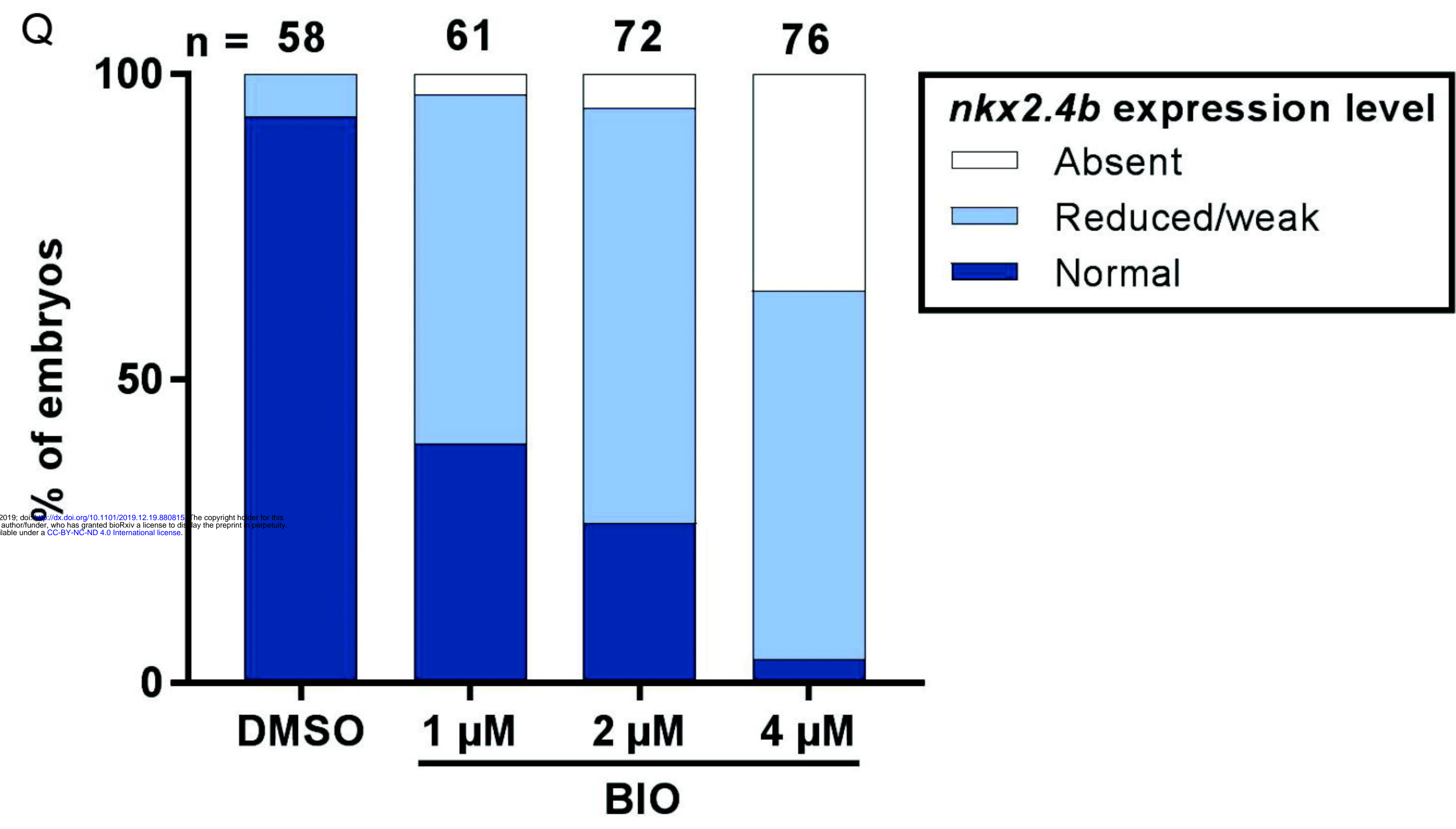
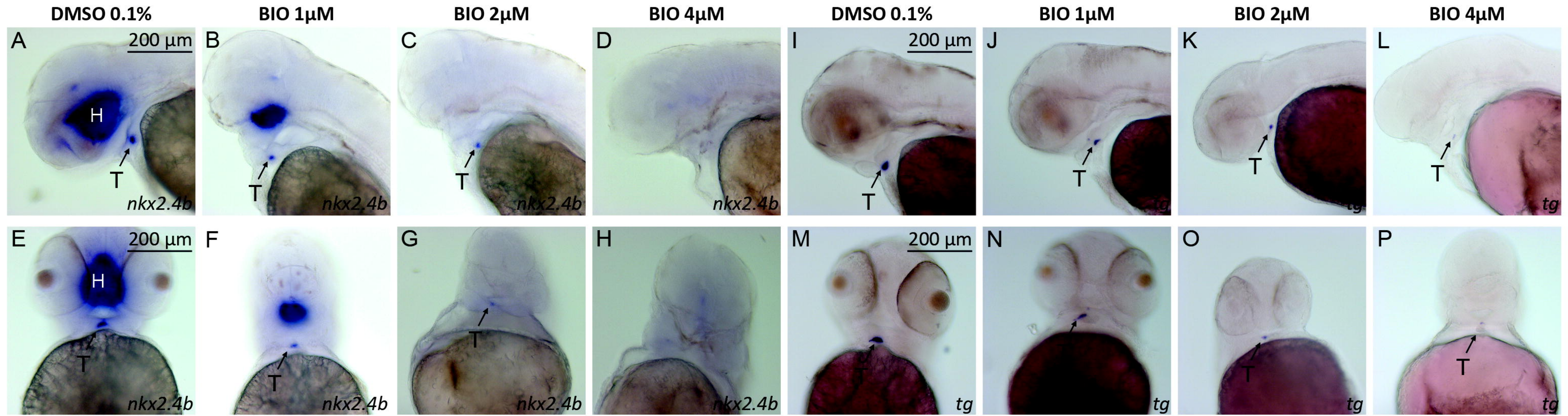
1162

1163

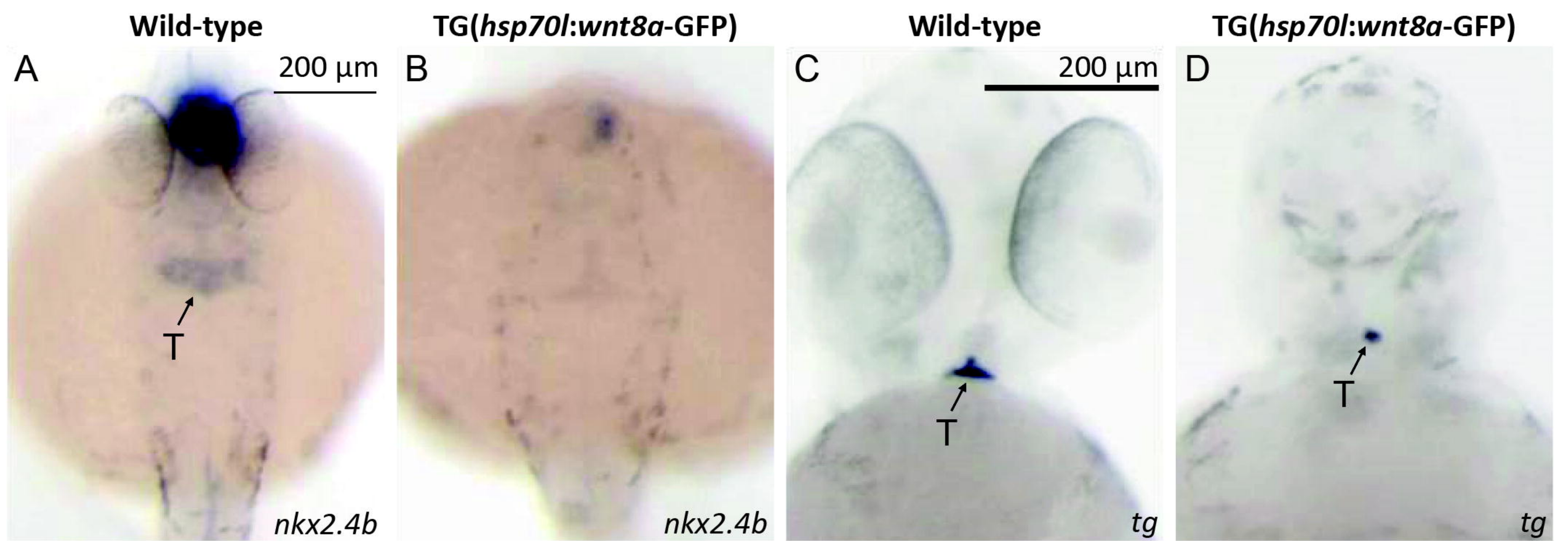


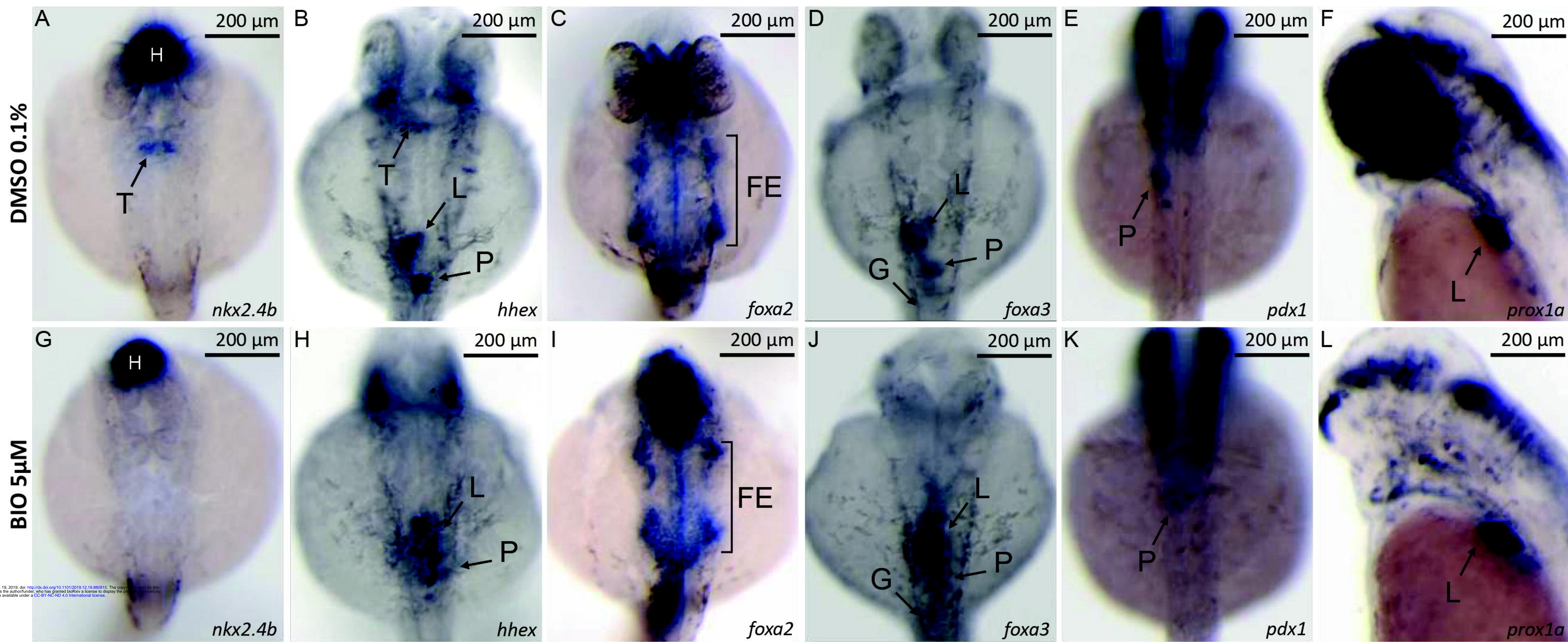
BIO treatment: 6-10 hpf

BIO treatment: 6-10 hpf



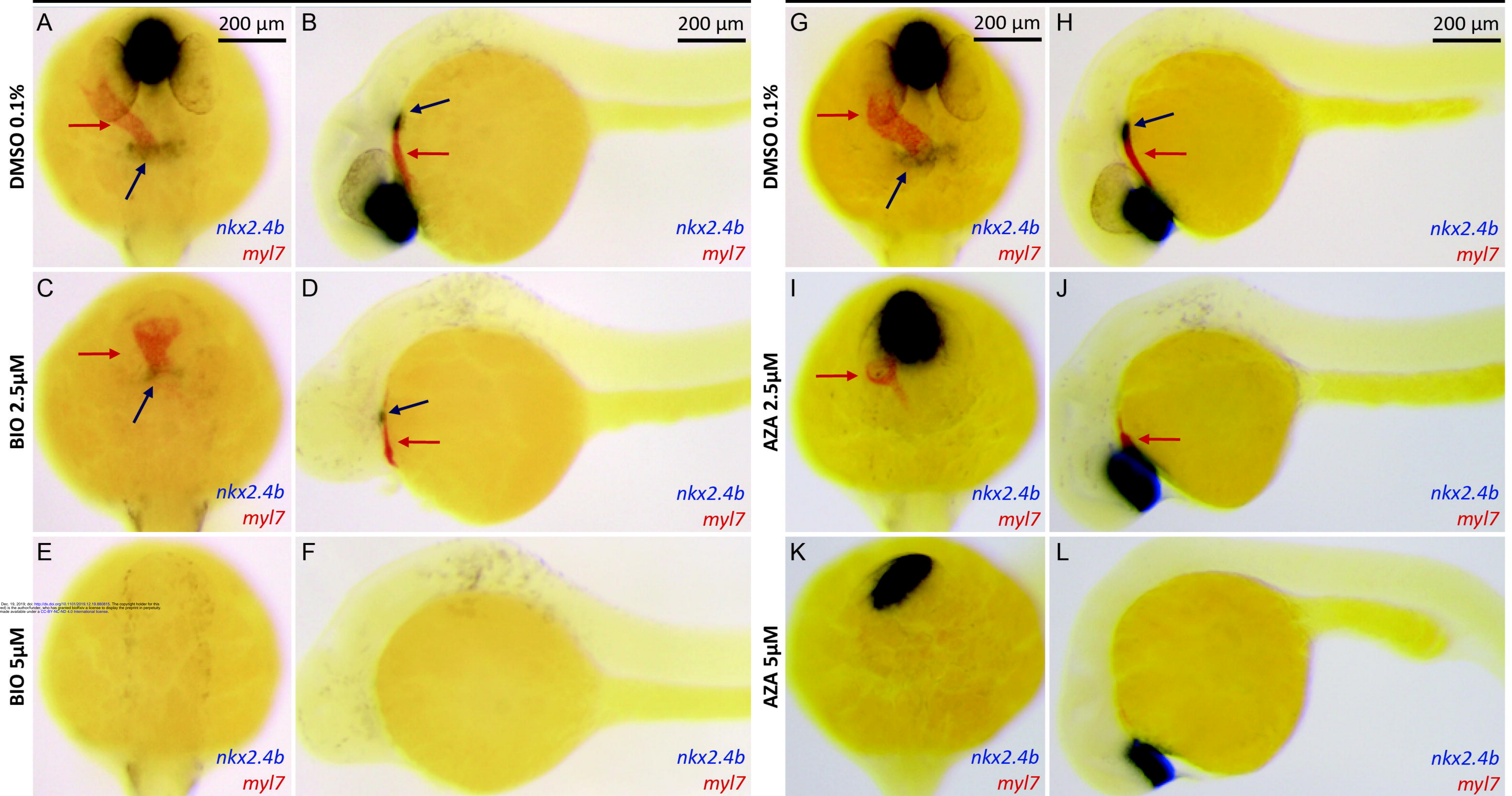
bioRxiv preprint first posted online Dec 19, 2015; doi: <https://doi.org/10.1101/018112>; this version posted Dec 19, 2015. The copyright holder for this preprint (which was not certified by peer review) is the author/funder, who has granted bioRxiv a license to display the preprint in perpetuity. It is made available under aCC-BY-ND 4.0 International license.



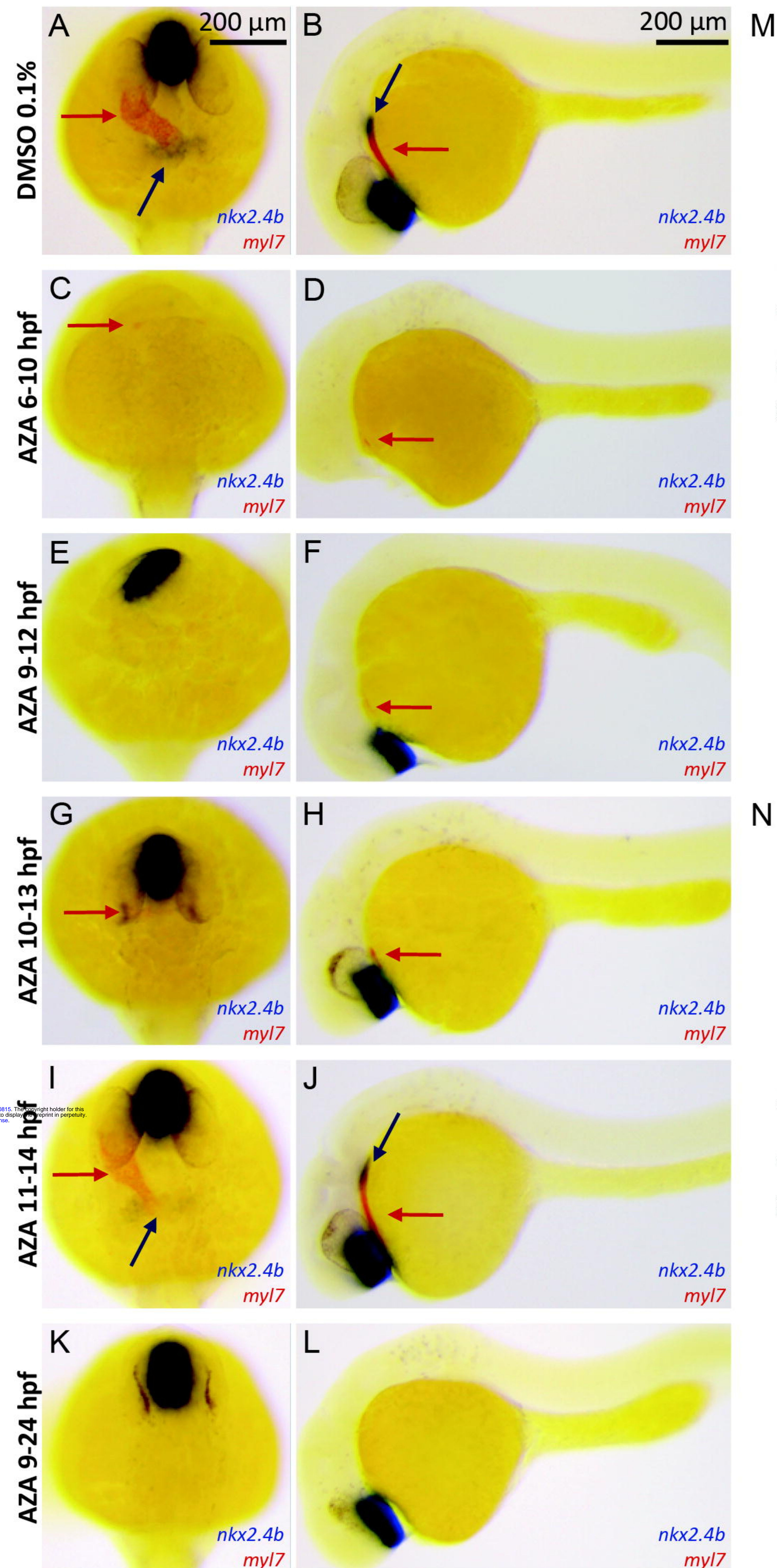


BIO treatment: 6-10 hpf

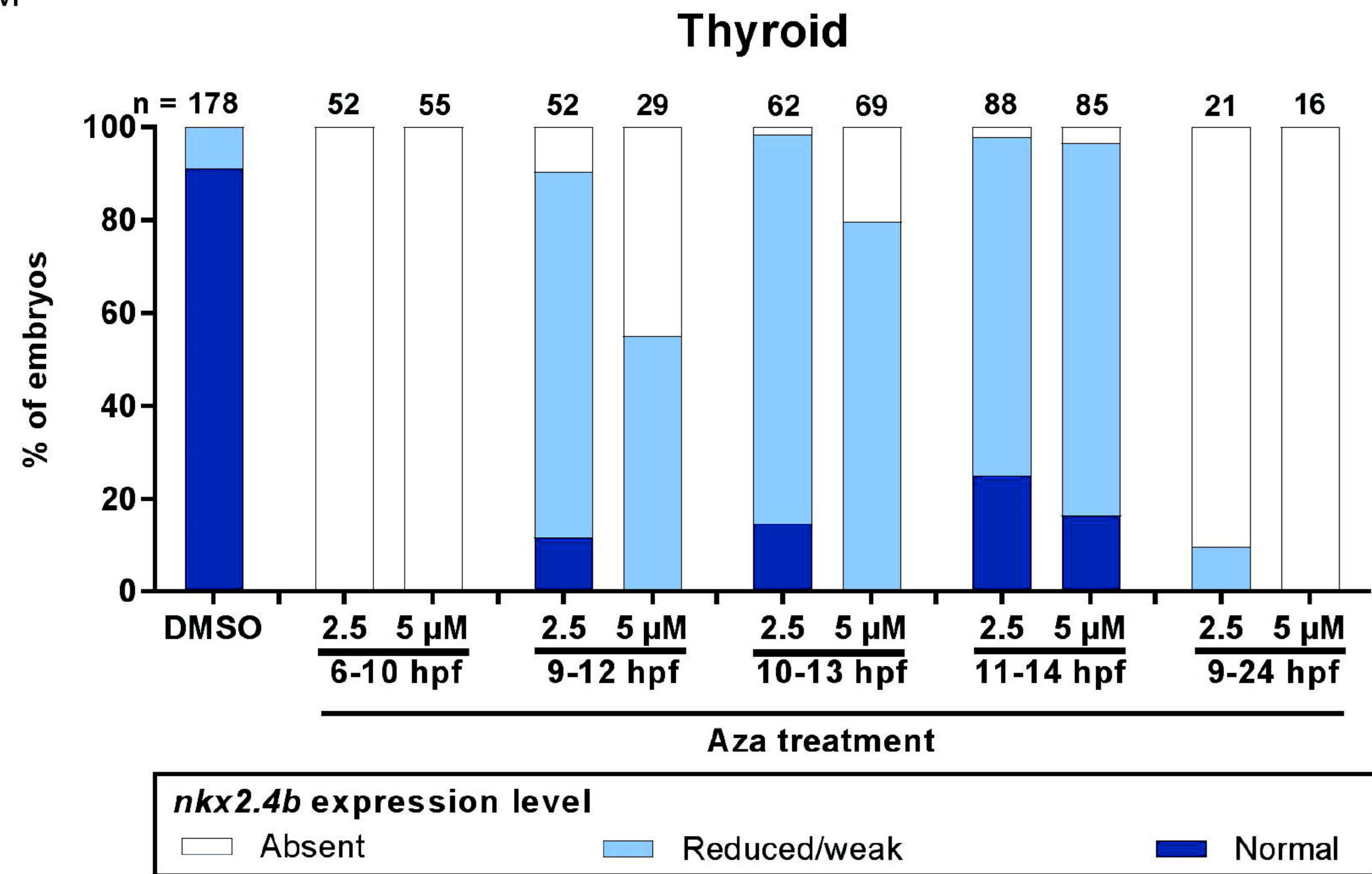
AZA treatment: 9-12 hpf



bioRxiv preprint first posted online Dec 19, 2015; doi: <https://doi.org/10.1101/031010>. The copyright holder for this preprint (which was not certified by peer review) is the author/funder, who has granted bioRxiv a license to display the preprint in perpetuity. It is made available under aCC-BY-NC-ND 4.0 International license.



M



N

